Geomechanics and Engineering, *Vol. 21, No. 5 (2020) 471-487*
DOI: https://doi.org/10.12989/gae.2020.21.5.471

A novel four-unknown integral model for buckling response of FG sandwich plates resting on elastic foundations under various boundary conditions using Galerkin's approach

Sara Chelahi Chikr[1,2], Abdelhakim Kaci[1,3], Abdelmoumen Anis Bousahla[4,5], Fouad Bourada[3,4,6], Abdeldjebbar Tounsi[3,4], E.A. Adda Bedia[4], S.R. Mahmoud[7], Kouider Halim Benrahou[3,4] and Abdelouahed Tounsi*[3,4]

[1]*Department of Civil and Hydraulic Engineering, Dr Tahar Moulay University, Faculty of Technology, BP 138 Cité En-Nasr 20000, Saida, Algeria*
[2]*Water Resources and Environment Laboratory, Dr Tahar Moulay University, BP 138 Cité En-Nasr 20000, Saida, Algeria*
[3]*Material and Hydrology Laboratory, University of Sidi Bel Abbes, Faculty of Technology, Civil Engineering Department, Algeria*
[4]*Department of Civil and Environmental Engineering, King Fahd University of Petroleum & Minerals, 31261 Dhahran, Eastern Province, Saudi Arabia*
[5]*Multi-scale Modeling and Simulation Laboratory, University of Sidi Bel Abbés, Algeria*
[6]*Department of Science and Technology, Tissemsilt University Center, BP 38004 Ben Hamouda, Algeria*
[7]*GRC Department, Jeddah Community College, King Abdulaziz University, Jeddah, Saudi Arabia*

(Received March 11, 2020, Revised April 18, 2020, Accepted April 24, 2020)

Abstract. In this work, the buckling analysis of material sandwich plates based on a two-parameter elastic foundation under various boundary conditions is investigated on the basis of a new theory of refined trigonometric shear deformation. This theory includes indeterminate integral variables and contains only four unknowns in which any shear correction factor not used, with even less than the conventional theory of first shear strain (FSDT). Applying the principle of virtual displacements, the governing equations and boundary conditions are obtained. To solve the buckling problem for different boundary conditions, Galerkin's approach is utilized for symmetric EGM sandwich plates with six different boundary conditions. A detailed numerical study is carried out to examine the influence of plate aspect ratio, elastic foundation coefficients, ratio, side-to-thickness ratio and boundary conditions on the buckling response of FGM sandwich plates. A good agreement between the results obtained and the available solutions of existing shear deformation theories that have a greater number of unknowns proves to demonstrate the precision of the proposed theory.

Keywords: buckling sandwich plates; functionally graded materials; new four-unknown refined shear deformation theory and various boundary conditions

1. Introduction

In structural analysis, the sandwich panels are composed of a core glued to two thin and rigid skins presenting the delaminating problems at the bonding interfaces due to the sudden change of the properties of the materials between the layers. To overcome this problem, sandwich structures of material with gradients of properties (FG) have been proposed in which the core or two skins can be made from materials with gradient properties (FGM).Functionally graded materials (FGM) are microscopically inhomogeneous composites produced by a gradual variation in the volume fractions of constituents (Koizumi 1997).The properties of materials vary progressively from one surface to another, thus eliminating the stress concentration of laminated composites. These special features make them preferable to conventional delaminating composite materials for applications in various structures, e.g., ships, submarines, aerospace vehicles, marine and civil structures (Wang and Shen 2013, Shen and Yang 2014, Madani *et al.* 2016, Li and Yang 2016, Ahmed *et al.* 2019, Avcar 2019), which are subject to various types such as bending, vibration, axial compression and thermal gradients, the static, dynamic and thermal responses of FGM plates that have been the subject of numerous research activities. The introduction of a FGM core combined with ceramic and metal protective sheets reduces the deformations of sandwich structures. Because of the wide range of applications of FGM in different engineering structures, it is very important to study the flanking behavior of FGM structures for proper analysis and design.

The remarkable advantages of the FGM thus accelerated the incorporation of these FGM into sandwich structures. Due to the widespread use of FGM sandwich structures in engineering, many studies have been developed to study buckling behavior which is considered to be one of the critical design factors of compression plates. Therefore, it is important to elucidate the buckling characteristics of FGM sandwich plates for optimal use in accurate and reliable

*Corresponding author, Ph.D.
E-mail: tou_abdel@yahoo.com

ISSN: 2005-307X (Print), 2092-6219 (Online)

design.

A number of analytical and numerical analyzes were performed to study the responses to isotropic and sandwich FGM plates. Zenkour (2005) investigated the buckling and free vibration of the functionally supported sinusoidal shear deformation plate theory (SSDPT). Matsunaga (2008) presented the free vibration and stability of plates functionally classified according to a 2D higher order deformation theory. Zhao *et al.* (2009) studied the mechanical and thermal buckling analysis of FGM plates. Das *et al.* (2006) presented a new triangular finite element based on a monolayer theory for modeling thick sandwich panels with or without calibrated core functionally subjected to thermomechanical loading. Anderson (2003) presented a three-dimensional elastic solution analytical method for a sandwich composite with a functional level core, subjected to transverse loading by a rigid spherical indenter. An exact thermoelasticity solution for a two-dimensional sandwich structure with a functional level coating was presented by Shodja *et al.* (2007). Xiang *et al.* (2011) has developed an order n model for free vibratory analysis of composite and sandwich plates. Neves and his co-workers (Neves *et al.* 2012a, b, c, d and 2013) presented static, free vibration and buckling analyzes of isotropic and sandwiched plates with different models of higher order shear deformation theories. Yaghoobi and Yaghoobi (2013) presented analytical solutions for the buckling of symmetric sandwich plates with FGM face sheets resting on an elastic foundation based on the first-order shear deformation plate theory (FSDPT) and submitted to mechanical, thermal, and thermo-mechanical loads. The prediction of nonlinear eigenfrequency of laminated curved sandwich structure using higher-order equivalent single-layer model has been presented by Katariya *et al.* (2017). Recently, several higher order shear deformation theories are proposed to examine the different behaviors of structures such as (Kolahchi and Moniri Bidgoli 2016, Kolahchi *et al.* 2017a, Kolahchi and Cheraghbak 2017, Hajmohammad *et al.* 2017 and 2018a, b, c, Kolahchi 2017, Golabchi *et al.* 2018, Fakhar and Kolahchi 2018, Hosseini and Kolahchi 2018, Belkacem *et al.* 2018, Hamidi *et al.* 2018, Ebrahimi and Barati 2018 and 2019, Abdelmalek *et al.* 2019, Safa *et al.* 2019, Sahouane *et al.* 2019, Zouatnia *et al.* 2019, Hadji *et al.* 2019, Kolahchi *et al.* 2019, Ebrahimi *et al.* 2019, Hajmohammad *et al.* 2019, Azmi *et al.* 2019, Akbas 2019a, b, Fenjan *et al.* 2019, Al-Maliki *et al.* 2019, Alasadi *et al.* 2019, Keshtegar *et al.* 2020a, b, Farrokhian and Kolahchi 2020, Eltaher and Mohamed 2020, Hamed *et al.* 2020, Barati and Shahverdi 2020).

Plates based on elastic foundations have been widely adopted by many researchers to model various engineering problems in recent decades. To describe the interactions of the plate and the foundation in the most appropriate way possible, scientists have proposed different types of foundation models. Winkler's elastic foundation model, which comprises an infinite number of separate springs without coupling effects between them, which leads to the disadvantage of a discontinuous deflection on the interacting surface of the plate, is a one-parameter model that is widely used in practice. This was later improved by Pasternak who took into account the interactions between the separate springs in the Winkler model by introducing a new dependent parameter. From that moment, the Pasternak model has been widely used to describe the mechanical behavior of structure-foundation interactions (Omurtag *et al.* 1997, Matsunaga 2000, Filipich and Rosales 2002, Zhou *et al.* 2004, Behravan Rad 2012).

This work aims to develop an efficient and simple theory of refined shear deformation for elastic base EGM sandwich plate buckling analyzes, taking into account various types of boundary conditions. The proposed theories contain four unknowns and motion equations than first-order shear deformation theory, but satisfy the equilibrium conditions at the upper and lower surfaces of the plate without the use of shear correction factors. The displacement field of the proposed theory is chosen as a function of the nonlinear variation of displacements in the plane through the thickness. It is assumed that the material properties of the faces of the sandwich plates vary in thickness direction only according to a new exponential distribution law in terms of volume fractions of the constituents. The central layer is always homogeneous and consists of an isotropic material. The analytical equations of the plate are obtained using Galerkin's method for different boundary conditions. The accuracy of the solutions obtained is verified by comparing the current results with those predicted by the solutions available in the literature.

2. Theoretical formulation

2.1 Modeling of functionally graded material

Consider a composite structure made of three isotropic layers of arbitrary thickness h, length a and width b. The FGM sandwich plate is supported at four edges defined in the (x,y,z) coordinate system with x- and y-axes located in the middle plane (z=0) and its origin placed at the corner of the plate. The vertical positions of the two interfaces between the core and faces layers are denoted, respectively, by h_1 and h_2. The sandwich core is a ceramic material and skins are composed of a functionally graded material across the thickness direction. The bottom skin varies from a metal-rich surface $\left(z = h_0 = -h/2\right)$ to a ceramic-rich surface while the top skin face varies from a ceramic-rich surface to a metal-rich surface $\left(z = h_3 = h/2\right)$. It is assumed to be rested on a Winkler–Pasternak type elastic foundation with the Winkler stiffness of k_w and shear stiffness of k_s as illustrated in Fig. 1. The volume fraction of the ceramic phase is obtained from a simple rule of mixtures as:

$$\begin{aligned} V^{(1)} &= \left(\frac{z-h_0}{h_1-h_0}\right)^p, && z \in \left[h_0, h_1\right] \\ V^{(2)} &= 1, && z \in \left[h_1, h_2\right] \\ V^{(3)} &= \left(\frac{z-h_3}{h_2-h_3}\right)^p, && z \in \left[h_2, h_3\right] \end{aligned} \tag{1}$$

where $V^{(n)}$, (n =1, 2, 3), denotes the volume fraction function of layer n; p is the volume fraction index

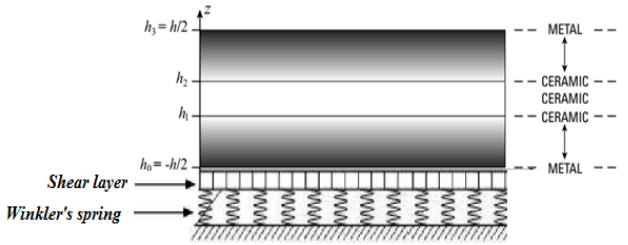

Fig. 1 Sandwich with isotropic core and FGM skins resting on elastic foundations

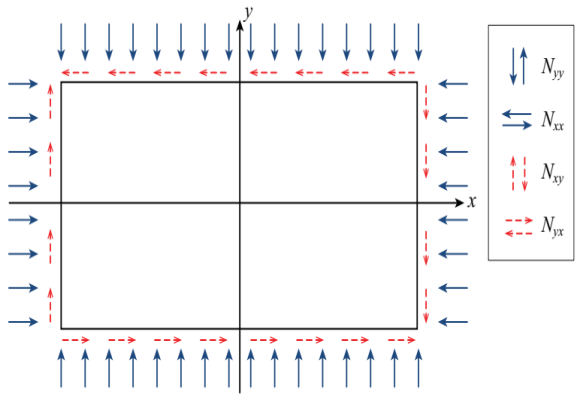

Fig. 2 Rectangular plate subjected to in-plane forces (Neves *et al.* 2012e)

$(0 \le p \le +\infty)$, which dictates the material variation profile through the thickness. Note that the core of the present sandwich and any isotropic material can be obtained as a particular case of the power-law function by setting p=0. The volume fraction for the metal phase is given as V_m=1−V_c.

The mechanical properties of functionally graded materials are often being represented in the exponentially graded form and power law variations one (Sobhy 2013). Based on an exponential law distribution, the Young's modulus $E^{(n)}(z)$ of the E-FGM is determined as:

$$E^{(n)}(z) = E_m \exp\left(\Re V^{(n)}\right), \quad \Re = \ln\left(E_c/E_m\right), \quad (n=1,2,3) \tag{2}$$

Poisson's ratio v is assumed to be a constant value through the sandwich plate thickness.

The sandwich plate is subjected to compressive in-plane forces acting on the mid-plane of the plate. $\bar{N}_{xx}$ and $\bar{N}_{yy}$ denote the in-plane loads perpendicular to the edges x = 0 and y = 0 respectively, and $\bar{N}_{xy}$ denotes the distributed shear force parallel to the edges x = 0 and y = 0 respectively (see Fig. 2).

2.2 A new four-unknown shear deformation theory

2.2.1 Kinematics and constitutive equations

In this study, further simplifying supposition are made to the conventional HSDT so that the number of unknowns is reduced. The displacement field of the conventional HSDT is given by:

$$\begin{aligned} u(x,y,z,t) &= u_0(x,y) - z\frac{\partial w_0}{\partial x} + f(z)\varphi_x \\ v(x,y,z,t) &= v_0(x,y) - z\frac{\partial w_0}{\partial y} + f(z)\varphi_y \\ w(x,y,z) &= w_0(x,y) \end{aligned} \tag{3}$$

$u_0, v_0, w_0, \varphi_x, \varphi_y$ are the five unknown displacement of the mid-plane of the plate. By considering that $\varphi_x = k_1\int\theta(x,y)\,dx$ and $\varphi_y = k_2\int\theta(x,y)\,dy$. The displacement fields mentioned above can be written as follows:

$$\begin{aligned} u(x,y,z) &= u_0(x,y) - z\frac{\partial w_0}{\partial x} + k_1 f(z)\int\theta(x,y)\,dx \\ v(x,y,z) &= v_0(x,y) - z\frac{\partial w_0}{\partial y} + k_2 f(z)\int\theta(x,y)\,dy \\ w(x,y,z) &= w_0(x,y) \end{aligned} \tag{4}$$

The constants k_1 and k_2 depends on the geometry. The shape functions $f(z)$ are chosen to satisfy the stress-free boundary conditions on the top and bottom surfaces of the plate, thus a shear correction factor is not required. In this study, the shape function is considered.

$$f(z) = \frac{z\left(\pi + 2\cos\left(\frac{\pi z}{h}\right)\right)}{(2+\pi)} \tag{5}$$

The nonzero linear strains are

$$\begin{Bmatrix}\varepsilon_x\\ \varepsilon_y\\ \gamma_{xy}\end{Bmatrix} = \begin{Bmatrix}\varepsilon_x^0\\ \varepsilon_y^0\\ \gamma_{xy}^0\end{Bmatrix} + z\begin{Bmatrix}k_x^b\\ k_y^b\\ k_{xy}^b\end{Bmatrix} + f(z)\begin{Bmatrix}k_x^s\\ k_y^s\\ k_{xy}^s\end{Bmatrix}, \quad \begin{Bmatrix}\gamma_{yz}\\ \gamma_{xz}\end{Bmatrix} = g(z)\begin{Bmatrix}\gamma_{yz}^0\\ \gamma_{xz}^0\end{Bmatrix} \tag{6}$$

where

$$\begin{Bmatrix}\varepsilon_x^0\\ \varepsilon_y^0\\ \gamma_{xy}^0\end{Bmatrix} = \begin{Bmatrix}\frac{\partial u_0}{\partial x}\\ \frac{\partial v_0}{\partial y}\\ \frac{\partial u_0}{\partial y} + \frac{\partial v_0}{\partial x}\end{Bmatrix}, \quad \begin{Bmatrix}k_x^b\\ k_y^b\\ k_{xy}^b\end{Bmatrix} = \begin{Bmatrix}-\frac{\partial^2 w_0}{\partial x^2}\\ -\frac{\partial^2 w_0}{\partial y^2}\\ -2\frac{\partial^2 w_0}{\partial x\partial y}\end{Bmatrix} \tag{7a}$$

$$\begin{Bmatrix}\gamma_{yz}^0\\ \gamma_{xz}^0\end{Bmatrix} = \begin{Bmatrix}k_2\int\theta\,dy\\ k_1\int\theta\,dx\end{Bmatrix} \tag{7b}$$

and $g(z)$ is given as follows

$$g(z) = f'(z) \tag{8}$$

The integrals defined in the above equations shall be resolved by considering the following relations

Table 1 Values of A', B', k_1 and k_2 for different boundary conditions

Boundary conditions	A'	k_1	B'	k_2
SSSS	$-\frac{1}{\lambda^2}$	λ^2	$-\frac{1}{\mu^2}$	μ^2
CSSS	$-\frac{1}{3\lambda^2}$	$3\lambda^2$	$-\frac{1}{\mu^2}$	μ^2
CSCS	$-\frac{1}{3\lambda^2}$	$3\lambda^2$	$-\frac{1}{3\mu^2}$	$3\mu^2$
CCSS	$-\frac{1}{4\lambda^2}$	$4\lambda^2$	$-\frac{1}{\mu^2}$	μ^2
CCCC	$-\frac{1}{4\lambda^2}$	$4\lambda^2$	$-\frac{1}{4\mu^2}$	$4\mu^2$
FFCC	$-\frac{1}{8\lambda^2}$	$8\lambda^2$	$-\frac{1}{4\mu^2}$	$4\mu^2$

where λ and μ are defined in section 3

$$\int \theta\, dx = A'\frac{\partial \theta}{\partial x};\ \int \theta\, dy = B'\frac{\partial \theta}{\partial y};$$
$$k_1 A'\frac{\partial \theta(x,y)}{\partial x} = \phi_x(x,y)\ ;\ k_2 B'\frac{\partial \theta(x,y)}{\partial y} = \phi_y(x,y) \tag{9}$$

where the coefficients A' and B' are expressed according to the type of solution used, in this case for Exact solutions for sandwich plates for different boundary conditions. Therefore, A', B', k_1 and k_2 are expressed in Table 1.

For elastic and isotropic FGMs, the constitutive relations can be written as:

$$\begin{Bmatrix}\sigma_x\\ \sigma_y\\ \tau_{xy}\end{Bmatrix}^{(n)} = \begin{bmatrix}Q_{11} & Q_{12} & 0\\ Q_{12} & Q_{22} & 0\\ 0 & 0 & Q_{66}\end{bmatrix}^{(n)} \begin{Bmatrix}\varepsilon_x\\ \varepsilon_y\\ \gamma_{xy}\end{Bmatrix}^{(n)} \text{ and}$$
$$\begin{Bmatrix}\tau_{yz}\\ \tau_{zx}\end{Bmatrix}^{(n)} = \begin{bmatrix}Q_{44} & 0\\ 0 & Q_{55}\end{bmatrix}^{(n)} \begin{Bmatrix}\gamma_{yz}\\ \gamma_{zx}\end{Bmatrix}^{(n)} \tag{10}$$

where (σ_x, σ_y σ_y, τ_{xy}, τ_{yz}, τ_{yx}) and (ε_x, ε_y, γ_{xy}, γ_{yz}, γ_{yx}) are the stress and strain components, respectively. Using the material properties defined in Eq. (1), stiffness coefficients, Q_{ij}, can be expressed as

$$Q_{11}^{(n)} = Q_{22}^{(n)} = \frac{E^{(n)}(z)}{1-\nu^2}, \tag{11a}$$

$$Q_{12}^{(n)} = \frac{\nu\, E^{(n)}(z)}{1-\nu^2}, \tag{11b}$$

$$Q_{44}^{(n)} = Q_{55}^{(n)} = Q_{66}^{(n)} = \frac{E^{(n)}(z)}{2(1+\nu)}, \tag{11c}$$

The stress and moment resultants of the FGM sandwich plate can be obtained by integrating Eq. (10) over the thickness, and are written as

$$\begin{Bmatrix}N_x, & N_y, & N_{xy}\\ M_x, & M_y, & M_{xy}\\ S_x, & S_y, & S_{xy}\end{Bmatrix} = \sum_{n=1}^{3}\int_{h_{n-1}}^{h_n} \left(\sigma_x,\sigma_y,\tau_{xy}\right)^{(n)} \begin{Bmatrix}1\\ z\\ f(z)\end{Bmatrix} dz, \tag{12a}$$

$$\begin{Bmatrix}N_x, & N_y, & N_{xy}\\ M_x, & M_y, & M_{xy}\\ S_x, & S_y, & S_{xy}\end{Bmatrix} = \sum_{n=1}^{3}\int_{h_{n-1}}^{h_n} \left(\sigma_x,\sigma_y,\tau_{xy}\right)^{(n)} \begin{Bmatrix}1\\ z\\ f(z)\end{Bmatrix} dz, \tag{12b}$$

where h_n and h_{n-1} are the top and bottom z-coordinates of the nth layer.

Using Eq. (10) in Eqs. (12), the stress resultants of a sandwich plate made up of three layers can be related to the total strains by

$$\begin{Bmatrix}N\\ M\\ S\end{Bmatrix} = \begin{bmatrix}A & B & B^s\\ B & D & D^s\\ B^s & D^s & H^s\end{bmatrix} \begin{Bmatrix}\varepsilon\\ k^b\\ k^s\end{Bmatrix}, \quad Q = A^s\gamma, \tag{13}$$

where

$$N = \left\{N_x, N_y, N_{xy}\right\}^t, \quad M^b = \left\{M_x, M_y, M_{xy}\right\}^t, \quad M^s = \left\{S_x, S_y, S_{xy}\right\}^t \tag{14a}$$

$$\varepsilon = \left\{\varepsilon_x^0, \varepsilon_y^0, \gamma_{xy}^0\right\}^t, \quad k^b = \left\{k_x^b, k_y^b, k_{xy}^b\right\}^t, \quad k^s = \left\{k_x^s, k_y^s, k_{xy}^s\right\}^t \tag{14b}$$

$$A = \begin{bmatrix}A_{11} & A_{12} & 0\\ A_{12} & A_{22} & 0\\ 0 & 0 & A_{66}\end{bmatrix}, \quad B = \begin{bmatrix}B_{11} & B_{12} & 0\\ B_{12} & B_{22} & 0\\ 0 & 0 & B_{66}\end{bmatrix}, \tag{14c}$$

$$D = \begin{bmatrix}D_{11} & D_{12} & 0\\ D_{12} & D_{22} & 0\\ 0 & 0 & D_{66}\end{bmatrix},$$

$$B^s = \begin{bmatrix}B_{11}^s & B_{12}^s & 0\\ B_{12}^s & B_{22}^s & 0\\ 0 & 0 & B_{66}^s\end{bmatrix}, \quad D^s = \begin{bmatrix}D_{11}^s & D_{12}^s & 0\\ D_{12}^s & D_{22}^s & 0\\ 0 & 0 & D_{66}^s\end{bmatrix}, \tag{14d}$$

$$H^s = \begin{bmatrix}H_{11}^s & H_{12}^s & 0\\ H_{12}^s & H_{22}^s & 0\\ 0 & 0 & H_{66}^s\end{bmatrix}, \tag{14e}$$

$$S = \left\{Q_{yz}, Q_{xz}\right\}^t, \quad \gamma = \left\{\gamma_{yz}, \gamma_{xz}\right\}^t, \quad A^s = \begin{bmatrix}A_{44}^s & 0\\ 0 & A_{55}^s\end{bmatrix},$$

where A_{ij}, B_{ij}, etc., are the plate stiffness, defined by

$$\begin{Bmatrix} A_{11} & B_{11} & D_{11} & B_{11}^s & D_{11}^s & H_{11}^s \\ A_{12} & B_{12} & D_{12} & B_{12}^s & D_{12}^s & H_{12}^s \\ A_{66} & B_{66} & D_{66} & B_{66}^s & D_{66}^s & H_{66}^s \end{Bmatrix} = \sum_{n=1}^{3}\int_{h_{n-1}}^{h_n} Q_{11}^{(n)}\left(1, z, z^2, f(z), z\,f(z), f^2(z)\right)\begin{Bmatrix} 1 \\ \nu^{(n)} \\ \dfrac{1-\nu^{(n)}}{2} \end{Bmatrix} dz \tag{15a}$$

and

$$\left(A_{22}, B_{22}, D_{22}, B_{22}^s, D_{22}^s, H_{22}^s\right) = \left(A_{11}, B_{11}, D_{11}, B_{11}^s, D_{11}^s, H_{11}^s\right), \quad Q_{11}^{(n)} = \frac{E(z)}{1-\nu^2} \tag{15b}$$

$$A_{44}^s = A_{55}^s = \sum_{n=1}^{3}\int_{h_{n-1}}^{h_n} \frac{E(z)}{2(1+\nu)}\left[g(z)\right]^2 dz, \tag{15c}$$

2.3 Governing equations

The principle of virtual work is employed for buckling problem of FG sandwich plate. The principle can be expressed in analytical from as

$$\delta U + \delta U_F + \delta V = 0 \tag{16}$$

where δU is the virtual strain energy, δU_F additional strain energy induced by the elastic foundations and δV is the virtual work done by applied forces.

The virtual strain energy is expressed by

$$\begin{aligned}\delta U &= \int_A\int_{-h/2}^{h/2}\left(\sigma_x^{(n)}\delta\varepsilon_x + \sigma_y^{(n)}\delta\varepsilon_y + \tau_{xy}^{(n)}\delta\gamma_{xy} + \tau_{xz}^{(n)}\delta\gamma_{xz} + \tau_{yz}^{(n)}\delta\gamma_{yz}\right)dAdz \\ &= \int_A\Big[N_x\delta\,\varepsilon_x^0 + N_{xy}\delta\gamma_{xy}^0 + N_y\delta\,\varepsilon_y^0 + M_x\delta\,k_x^b + M_y\delta\,k_y^b \\ &\quad + M_{xy}\delta\,k_{xy}^b + S_x\delta\,k_x^s + S_y\delta\,k_y^s + S_{xy}\delta\,k_{xy}^s + Q_{yz}\delta\gamma_{yz}^0 + Q_{xz}\delta\gamma_{xz}^0\Big]dA\end{aligned} \tag{17}$$

where A is the top surface.

The strain energy induced by elastic foundations can be defined as

$$\delta U_F = \int_A f_e\delta w_0 dA \tag{18}$$

where A is the area of top surface and f_e is the density of reaction force of foundation. For the Pasternak foundation model

$$f_e = k_w w - k_{sx}\frac{\partial^2 w}{\partial x^2} - k_{sy}\frac{\partial^2 w}{\partial y^2} \tag{19}$$

where k_w is the modulus of subgrade reaction (elastic coefficient of the foundation) and k_{sx} and k_{sy} are the shear moduli of the subgrade (shear layer foundation stiffness). If foundation is homogeneous and isotropic, we will get $k_{sx} = k_{sy} = k_s$. If the shear layer foundation stiffness is neglected, Pasternak foundation becomes a Winkler foundation. If the shear layer foundation stiffness is neglected, Pasternak foundation becomes a Winkler foundation.

The external virtual work due to in-plane forces and shear forces applied to the plate is given as:

$$\delta V = -\int_A\left(\bar{N}_{xx}\frac{\partial^2 w_0}{\partial x^2} + 2\bar{N}_{xy}\frac{\partial^2 w_0}{\partial x\partial y} + \bar{N}_{yy}\frac{\partial^2 w_0}{\partial y^2}\right)\delta w_0 dA \tag{20}$$

Being $\bar{N}_{xx}$ and $\bar{N}_{yy}$ the in-plane loads perpendicular to the edges x=0 and y=0, respectively, and $\bar{N}_{xy}$ and $\bar{N}_{yx}$ the distributed shear forces parallel to the edges x=0 and y=0, respectively.

Substituting Eqs. (18), (19) and (20) into Eq. (16) and integrating by parts, and collecting the coefficients of $\left(\delta u_0, \delta v_0, \delta w_0, \delta\theta\right)$, the following equations of motion are obtained

$$\begin{aligned}&\delta u_0 : \frac{\partial N_x}{\partial x} + \frac{\partial N_{xy}}{\partial y} = 0 \\ &\delta v_0 : \frac{\partial N_y}{\partial y} + \frac{\partial N_{xy}}{\partial x} = 0 \\ &\delta w_0 : \frac{\partial^2 M_x}{\partial x^2} + 2\frac{\partial^2 M_{xy}}{\partial x\partial y} + \frac{\partial^2 M_y}{\partial y^2} - \bar{N} - f_e = 0 \\ &\delta\theta : -k_1 S_x - k_2 S_y - \left(k_1 A' + k_2 B'\right)\frac{\partial^2 S_{xy}}{\partial x\partial y} + k_1 A'\frac{\partial Q_{xz}}{\partial x} + k_2 B'\frac{\partial Q_{yz}}{\partial y} = 0\end{aligned} \tag{21}$$

2.4 Equations of motion in terms of displacements

Substituting Eqs. (7), (13) into Eq. (20), the equations of motion can be expressed in terms of generalized displacements $\left(\delta u_0, \delta v_0, \delta w_0, \delta\theta\right)$ as

$$\begin{aligned}&\delta u_0 : L_1 u_0 + A_{11}L_2 v_0 - L_3\frac{\partial w_0}{\partial x} + L_4\frac{\partial\theta}{\partial x} = 0 \\ &\delta v_0 : A_{11}L_2 u_0 + L_5 v_0 - L_3\frac{\partial w_0}{\partial y} + L_6\frac{\partial\theta}{\partial y} = 0 \\ &\delta w_0 : L_3\left(\frac{\partial u_0}{\partial x} + \frac{\partial v_0}{\partial y}\right) - L_7 w_0 + L_8\theta = 0 \\ &\delta\theta : -L_4\frac{\partial u_0}{\partial x} - L_6\frac{\partial v_0}{\partial y} + L_8 w_0 - L_9\theta = 0\end{aligned} \tag{22}$$

where the operator L_i are given by

$$L_1 = A_{11}\nabla_x^2,\ L_2 = \left(\nu + \bar{\nu}\right)\frac{\partial^2}{\partial x\partial y},\ L_3 = B_{11}\nabla^2,\ L_4 = B_{11}^s\left(k_1 + k_2\nu + \bar{\nu}\left(k_1 A' + k_2 B'\right)\frac{\partial^2}{\partial y^2}\right) \tag{22a}$$

$$L_5 = A_{11}\nabla_y^2,\quad L_6 = B_{11}^s\left(k_1\nu + k_2 + \bar{\nu}\left(k_1 A' + k_2 B'\right)\frac{\partial^2}{\partial x^2}\right) \tag{22b}$$

$$L_7 = D_{11}\nabla^4 + \left(\bar{N}_{xx}\frac{\partial^2}{\partial x^2} + 2\bar{N}_{xy}\frac{\partial^2}{\partial x\partial y} + \bar{N}_{yy}\frac{\partial^2}{\partial y^2} + k_w - k_s\nabla^2\right) \tag{22c}$$

Table 2 The admissible functions $X_m(x)$ and $Y_n(y)$

	Boundary conditions		The functions $X_m(x)$ and $Y_n(y)$	
SSSS	$X_m(0)=X''_m(0)=0$ $X_m(a)=X''_m(a)=0$	$Y_n(0)=Y''_n(0)=0$ $Y_n(b)=Y''_n(b)=0$	$\sin(\lambda x)$	$\sin(\mu y)$
CSSS	$X_m(0)=X'_m(0)=0$ $X_m(a)=X''_m(a)=0$	$Y_n(0)=Y''_n(0)=0$ $Y_n(b)=Y''_n(b)=0$	$\sin(\lambda x)[\cos(\lambda x)]-1$	$\sin(\mu y)$
CSCS	$X_m(0)=X'_m(0)=0$ $X_m(a)=X''_m(a)=0$	$Y_n(0)=Y'_n(0)=0$ $Y_n(b)=Y''_n(b)=0$	$\sin(\lambda x)[\cos(\lambda x)]-1$	$\sin(\mu y)[\cos(\mu y)]-1$
CCSS	$X_m(0)=X'_m(0)=0$ $X_m(a)=X'_m(a)=0$	$Y_n(0)=Y''_n(0)=0$ $Y_n(b)=Y''_n(b)=0$	$\sin^2(\lambda x)$	$\sin(\mu y)$
CCCC	$X_m(0)=X'_m(0)=0$ $X_m(a)=X'_m(a)=0$	$Y_n(0)=Y'_n(0)=0$ $Y_n(b)=Y'_n(b)=0$	$\sin^2(\lambda x)$	$\sin^2(\mu y)$
FFCC	$X''_m(0)=X'''_m(0)=0$ $X''_m(a)=X'''_m(a)=0$	$Y_n(0)=Y'_n(0)=0$ $Y_n(b)=Y'_n(b)=0$	$\cos^2(\lambda x)[\sin^2(\lambda x)]-1$	$\sin^2(\mu y)$

( )' denotes the derivative with respect to the corresponding coordinates

$$L_8 = D_{11}^s \left(\begin{array}{l} \left(k_1+k_2\nu\right)\dfrac{\partial^2}{\partial x^2}+2\bar{\nu}\left(k_1A'+k_2B'\right)\dfrac{\partial^4}{\partial x^2\partial y^2} \\ +\left(k_1\nu+k_2\right)\dfrac{\partial^2}{\partial y^2} \end{array} \right) \tag{22d}$$

$$L_9 = H_{11}^s\left(k_1^2+2\nu k_1k_2+k_2^2\right)+\bar{\nu}H_{11}^s\left(k_1A'+k_2B'\right)^2\frac{\partial^4}{\partial x^2\partial y^2} -k_1{}^2A'^2A_{55}^s\frac{\partial^2}{\partial x^2}-k_2{}^2B'^2A_{55}^s\frac{\partial^2}{\partial y^2} \tag{22e}$$

in which

$$\nabla_x^2=\frac{\partial^2}{\partial x^2}+\bar{\nu}\frac{\partial^2}{\partial y^2}, \quad \nabla_y^2=\bar{\nu}\frac{\partial^2}{\partial x^2}+\frac{\partial^2}{\partial y^2}, \quad \nabla^2=\frac{\partial^2}{\partial x^2}+\frac{\partial^2}{\partial y^2}, \quad \nabla^4=\nabla^2\left(\nabla^2\right), \quad \bar{\nu}=\frac{1-\nu}{2} \tag{23}$$

3. Exact solutions for FGMs sandwich plates

In this section, exact solutions of the governing equations for buckling analysis of a EGMs sandwich plate with simply supported (S), clamped (C) or free (F) edges are presented. These boundary conditions are defined as follow:

Simply supported (S)

$$\begin{aligned} &v_0=w_0=\frac{\partial\theta}{\partial y}=N_{xx}=M_{xx}=S_{xx}=0 \qquad at \qquad x=0,a, \\ &u_0=w_0=\frac{\partial\theta}{\partial x}=N_{yy}=M_{yy}=S_{yy}=0 \qquad at \qquad y=0,b. \end{aligned} \tag{24}$$

Clamped (C):

$$u_0=v_0=w_0=\frac{\partial\theta}{\partial x}=\frac{\partial\theta}{\partial y}=0 \quad at \quad x=0,a; \quad y=0,b. \tag{25}$$

Free (F):

$$\begin{aligned} &M_{xx}=M_{xy}=Q_{xz}=0 \qquad at \qquad x=0,a, \\ &M_{yy}=M_{xy}=Q_{yz}=0 \qquad at \qquad y=0,b. \end{aligned} \tag{26}$$

The following representation for the displacement quantities, that satisfy the above boundary conditions, is appropriate in the case of our problem:

$$\begin{Bmatrix} u_0 \\ v_0 \\ w_0 \\ \theta \end{Bmatrix} = \sum_{m=1}^{\infty}\sum_{n=1}^{\infty} \begin{Bmatrix} U_{mn}\dfrac{\partial X_m(x)}{\partial x}Y_n(y) \\ V_{mn}X_m(x)\dfrac{\partial Y_n(y)}{\partial y} \\ W_{mn}X_m(x)Y_n(y) \\ Z_{mn}\dfrac{\partial^2 X_m(x)}{\partial x^2}Y_n(y) \end{Bmatrix} \tag{27}$$

where U_{mn}, V_{mn}, W_{mn} and Z_{mn} are arbitrary coefficients to be determined. The functions $X_m(x)$ and $Y_n(y)$ are suggested here to satisfy at least the geometric boundary conditions given in Eqs. (24)-(26) and represent approximate shapes of the deflected surface of the plate. These functions, for the different cases of boundary conditions, are listed in Table 2 noting that $\lambda=m\pi/a$, $\mu=n\pi/b$. The plate is subjected to an in-plane forces sin two directions $\bar{N}_x=N_{cr}$, $\bar{N}_y=\chi N_{cr}$ i.e., $\chi=\bar{N}_y/\bar{N}_x$ and $\bar{N}_{xy}=0$.

Substituting expressions (27) into the governing Eq. (22) and multiplying each equation by the corresponding eigenfunction then integrating over the domain of solution, we can obtain, after some mathematical manipulations, the following equations:

$$\begin{bmatrix} S_{11} & S_{12} & S_{13} & S_{14} \\ S_{21} & S_{22} & S_{23} & S_{24} \\ S_{31} & S_{32} & S_{33} & S_{34} \\ S_{41} & S_{42} & S_{43} & S_{44} \end{bmatrix} \begin{Bmatrix} U_{mn} \\ V_{mn} \\ W_{mn} \\ Z_{mn} \end{Bmatrix} = 0 \tag{28}$$

in which

$$\begin{aligned} S_{11}&=A_{11}\left(e_{12}+\bar{\nu}e_8\right) \\ S_{12}&=A_{11}\left(\nu+\bar{\nu}\right)e_8 \\ S_{13}&=-B_{11}\left(e_8+e_{12}\right) \end{aligned} \tag{29}$$

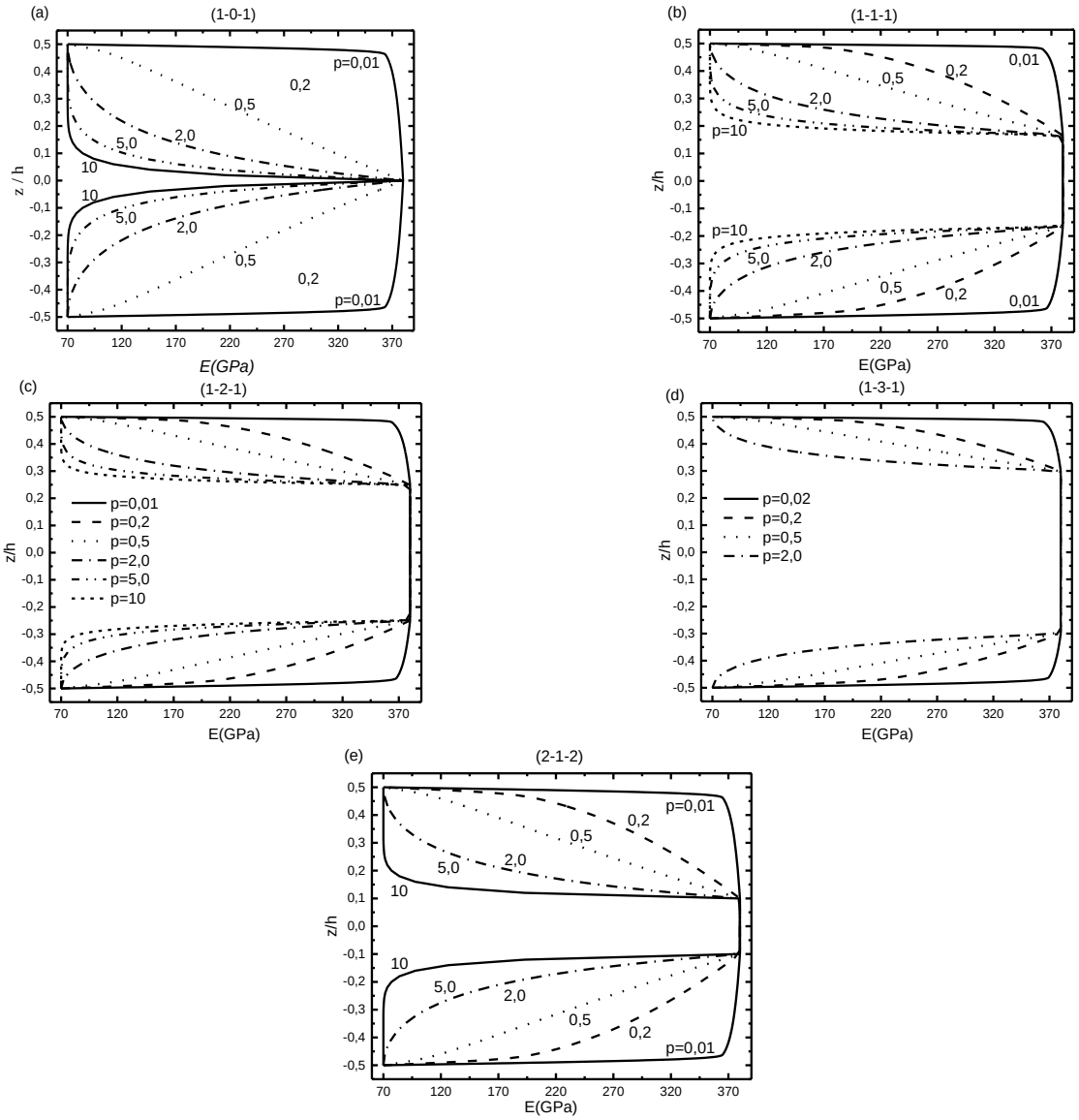

Fig. 3 Variation of the Young's modulus through plate thickness of symmetric sandwich plates for various values of the power-law index p: (a) The (1-0-1) EGM sandwich plate, (b) The (1-1-1) EGM sandwich plate, (c) The (1-2-1) EGM sandwich plate, (d) The (1-3-1) EGM sandwich plate and (e) The (2-1-2) EGM sandwich plate.

$$
\begin{aligned}
S_{14} &= B_{11}^{s}\left[(k_1+k_2\nu)e_{12}+\bar{\nu}(k_1A'+k_2B')e_{20}\right]\\
S_{21} &= A_{11}\left(\nu+\bar{\nu}\right)e_{10}\\
S_{22} &= A_{11}\left(\bar{\nu}e_{10}+e_4\right)\\
S_{23} &= -B_{11}\left(e_{10}+e_4\right)\\
S_{24} &= B_{11}^{s}\left[\left(k_1\nu+k_2\right)e_{10}+\bar{\nu}\left(k_1A'+k_2B'\right)e_{21}\right]\\
S_{31} &= -B_{11}\left(e_{13}+e_{11}\right)\\
S_{32} &= -B_{11}\left(e_{11}+e_5\right)\\
S_{33} &= D_{11}\left(e_{13}+e_5+2e_{11}\right)+\left(\bar{N}_{xx}-k_s\right)e_9+\left(\bar{N}_{yy}-k_s\right)e_3+k_we_1+2\bar{N}_{xy}e_7\\
S_{34} &= -D_{11}^{s}\left[\left(k_1+k_2\nu\right)e_{13}+2\bar{\nu}\left(k_1A'+k_2B'\right)e_{14}+\left(k_1\nu+k_2\right)e_{11}\right]\\
S_{41} &= B_{11}^{s}\left[\left(k_1+k_2\nu\right)e_{15}+\bar{\nu}\left(k_1A'+k_2B'\right)e_{16}\right]\\
S_{42} &= B_{11}^{s}\left[\left(k_1\nu+k_2\right)e_{17}+\bar{\nu}\left(k_1A'+k_2B'\right)e_{16}\right]\\
S_{43} &= -D_{11}^{s}\left[\left(k_1+k_2\nu\right)e_{15}+2\bar{\nu}\left(k_1A'+k_2B'\right)e_{16}+\left(k_1\nu+k_2\right)e_{17}\right]\\
S_{44} &= H_{11}^{s}\left(k_1^2+2\nu k_1k_2+k_2^2\right)e_{15}+\bar{\nu}H_{11}^{s}\left(k_1A'+k_2B'\right)^2e_{18}\\
&\quad -A_{55}^{s}\left(\left(k_1A'\right)^2e_{19}+\left(k_2B'\right)^2e_{16}\right)
\end{aligned}
\tag{29}
$$

with

$$
\begin{aligned}
(e_{20},e_8,e_{12}) &= \int_0^b\int_0^a\left(X_m'''Y_n'',X_m'Y_n'',X_m'''Y_n\right)X_m'Y_n\,dxdy\\
(e_{21},e_4,e_{10}) &= \int_0^b\int_0^a\left(X_m'''Y_n',X_mY_n''',X_m''Y_n'\right)X_mY_n'dxdy\\
(e_1,e_3,e_5,e_{14}) &= \int_0^b\int_0^a\left(X_mY_n,X_mY_n'',X_mY_n'''',X_m''''Y_n''\right)X_mY_n\,dxdy\\
(e_7,e_9,e_{11},e_{13}) &= \int_0^b\int_0^a\left(X_m'Y_n',X_m''Y_n,X_m''Y_n'',X_m''''Y_n\right)X_mY_n\,dxdy\\
(e_{15},e_{16},e_{17}) &= \int_0^b\int_0^a\left(X_m''Y_n,X_m''Y_n'',X_mY_n''\right)X_m''Y_n\,dxdy\\
(e_{18},e_{19}) &= \int_0^b\int_0^a\left(X_m''''Y_n'',X_m''''Y_n\right)X_m''Y_n\,dxdy
\end{aligned}
\tag{30}
$$

4. Numerical results and discussions

Table 3 Comparison of critical buckling load [$N_{cr}a^2/(D\pi^2)$] of a simply supported thin homogeneous square plate (a/h=1000, p=0) resting on Pasternak's elastic foundations (n=1, χ=0)

m	K_w	K_s	Sobhi (2013)	Present
1	0	0	3.99998	3.999977554
2	0	100	18.91506	18.91506029
1	100	0	5.02658	5.026575782
2	100	100	19.17171	19.17170985

Table 4 Comparison of critical buckling load [$N_{cr}b^2/D$] of a simply supported homogeneous plate (p=0) resting on Pasternak's elastic foundations (n=1, χ=0)

		(K_w, K_s)					
a/b	a/h	Sobhi(2013)			Present		
		(0,0)	(100,10)	(1000,100)	(0,0)	(100,10)	(1000,100)
0.5	1000	61.6848[1]	152.213[1]	704.589[2]	61.6848[1]	152.2133[1]	704.5888[2]
	100	61.6633[1]	152.192[1]	704.378[2]	61.6634[1]	152.1919[1]	704.3786[2]
	10	59.5887[1]	150.117[1]	685.567[2]	59.5965[1]	150.1250[1]	685.6363[2]
	5	54.0859[1]	144.614[1]	641.380[3]	54.1135[1]	144.6419[1]	641.9917[3]
1	1000	39.4782[1]	69.6103[1]	212.014[2]	39.4782[1]	69.6103[1]	212.0144[2]
	100	39.4562[1]	69.5883[1]	211.928[2]	39.4563[1]	69.5884[1]	211.9289[2]
	10	37.3753[1]	67.5074[1]	204.416[2]	37.3831[1]	67.5152[1]	204.4438[2]
	5	32.2398[1]	54.6116[2]	174.391[3]	32.2656[1]	54.6862[2]	174.5753[3]
2	1000	39.4775[2]	45.1108[2]	85.2562[3]	39.4775[2]	45.1108[2]	85.2562[3]
	100	39.3897[2]	45.0229[2]	85.0889[3]	39.3900[2]	45.0233[2]	85.0896[3]
	10	32.2398[2]	37.8581[3]	72.4117[4]	32.2656[2]	37.9010[3]	72.4863[4]
	5	19.0400[3]	22.6778[4]	52.2276[4]	19.1255[3]	22.8060[4]	52.3558[4]

Mode shape (m) is denoted by the superscript numbers

In this section, the accuracy of the presented plate theory for the buckling analysis of symmetric rectangular EGM sandwich plates resting on two-parameter elastic foundations with various cases of the boundary conditions is demonstrated by comparing the analytical solution with those of other available results in the literature.

The combination of materials consists of aluminum and alumina with the following material properties:

• Ceramic (alumina, Al_2O_3): $E_c = 380\ GPa, \nu_c = 0.3$

• Metal (aluminum, Al): $E_m = 70\ GPa, \nu_m = 0.3$

In the following, we note that several kinds of sandwich plates are used:

• The (1-0-1) FG sandwich plate: The plate is symmetric and made of only two equal-thickness FG layers, i.e., there is no core layer. Thus, we have, $h_1 = h_2 = 0$

• The (1-1-1) FG sandwich plate: Here, the plate is symmetric and made of three equal-thickness layers. In this case, we have, $h_1 = -h/6, h_2 = h/6$

• The (1-2-1) FG sandwich plate: The plate is symmetric and we have: $h_1 = -h/4, h_2 = h/4$

• The (1-3-1) FG sandwich plate: The plate is symmetric and we have: $h_1 = -3h/10, h_2 = 3h/10$

• The (2-1-2) FG sandwich plate, we have: $h_1 = -h/10, h_2 = h/10$.

Fig. 3 shows the through-the-thickness variation of the of Young's modulus for p=0.01, 0.2, 0.5, 2, 5 and 10.

For convenience, the following non-dimensional forms are used:

$$\overline{N}_{cr} = \frac{N_{cr}\, a^2}{100h^3}, \qquad K_w = \frac{k_w\, a^4}{D},$$

$$K_s = \frac{k_{sx}\, a^2}{D} = \frac{k_{sy}\, a^2}{D}, \qquad D = \frac{E_c h^3}{12(1-\nu^2)}$$

Many examples have been solved numerically using the following fixed data (unless otherwise stated) $a/h = 10, m = n = 1, K_w = K_s = 100, \chi = 1.$

The accuracy of a new four-unknown refined plate theory is validated by comparing the results with those available in the literature. The non-dimensionalized uniaxial buckling load for a simply supported thin homogeneous square plate without or resting on elastic foundations has been obtained. The results are presented in Table 3 and compared with those available in the literature (Sobhi 2013). It is seen that the results are in good agreement.

Table 4 shows the validation of the present outlined theory by comparing the present results of uniaxial critical buckling load for various values of the ratios a/b and a/h. It can be seen that the mean response values given by the present theory are almost same.

Table 5 Effects of elastic foundation stiffnesses k_w and k_s and side-to-thickness ratio *a/h* on the critical buckling $\overline{N}_{cr}$ of various types of simply supported sandwich square plates (p = 0.5)

Scheme	Theory	k_w=k_s=0			k_w=100, k_s=0			k_w=100, k_s=100		
		a/h=5	10	20	a/h=5	10	20	a/h=5	10	20
1-0-1	FPT[a]	2.5154	2.7987	2.8797	4.2783	4.5616	4.6427	39.0768	39.3601	39.4412
	TPT[a]	2.5592	2.8119	2.8832	4.3220	4.5748	4.6461	39.1206	39.3734	39.4447
	SPT[a]	2.5618	2.8127	2.8834	4.3247	4.5756	4.6463	39.1232	39.3741	39.4449
	EPT[a]	2.5652	2.8137	2.8837	4.3281	4.5766	4.6466	39.1266	39.3752	39.4451
	HPT[a]	2.5834	2.8193	2.8852	4.3463	4.5822	4.6481	39.1448	39.3808	39.4466
	Present	2.5647	2.8136	2.8837	4.3276	4.5765	4.6466	39.1261	39.3750	39.4451
1-1-1	FPT[a]	3.0560	3.4014	3.5003	4.8189	5.1643	5.2632	39.6175	39.9628	40.0617
	TPT[a]	3.1014	3.4151	3.5039	4.8643	5.1781	5.2668	39.6629	39.9766	40.0653
	SPT[a]	3.1030	3.4156	3.5040	4.8659	5.1785	5.2669	39.6644	39.9770	40.0655
	EPT[a]	3.1054	3.4163	3.5042	4.8683	5.1792	5.2671	39.6668	39.9777	40.0656
	HPT[a]	3.1399	3.4269	3.5070	4.9029	5.1898	5.2699	39.7014	39.9883	40.0684
	Present	3.1051	3.4162	3.5042	4.8680	5.1791	5.2671	39.6665	39.9777	40.0656
1-2-1	FPT[a]	3.4772	3.8906	4.0097	5.2401	5.6535	5.7726	40.0386	40.4520	40.5712
	TPT[a]	3.5165	3.9026	4.0129	5.2795	5.6655	5.7758	40.0780	40.4541	40.5744
	SPT[a]	3.5165	3.9026	4.0129	5.2795	5.6655	5.7758	40.0780	40.4640	40.5744
	EPT[a]	3.5176	3.9028	4.0130	5.2805	5.6657	5.7759	40.0790	40.4643	40.5744
	HPT[a]	3.5799	3.9220	4.0180	5.3429	5.6850	5.7810	40.1414	40.4835	40.5795
	Present	3.5174	3.9028	4.0130	5.2804	5.6657	5.7759	40.0789	40.4643	40.5745
1-3-1	FPT[a]	3.7922	4.2636	4.4004	5.5551	6.0265	6.1633	40.3537	40.8251	40.9618
	TPT[a]	3.8253	4.2738	4.4031	5.5882	6.0367	6.1660	40.3867	40.8353	40.9645
	SPT[a]	3.8243	4.2734	4.4030	5.5872	6.0364	6.1659	40.3857	40.8349	40.9644
	EPT[a]	3.8245	4.2735	4.4030	5.5875	6.0364	6.1659	40.3860	40.8349	40.9644
	HPT[a]	3.9214	4.3004	4.4101	5.6743	6.0634	6.1730	40.4728	40.8619	40.9716
	Present	3.8245	4.2735	4.4030	5.5874	6.0364	6.1659	40.3860	40.8349	40.9645

[a] Sobhy (2013). EPT: exponential shear deformation plate theory; FPT: first-order shear deformation plate theory; HPT: hyperbolic shear deformation plate theory; SPT: sinusoidal shear deformation plate theory; TPT: third-order shear deformation plate theory

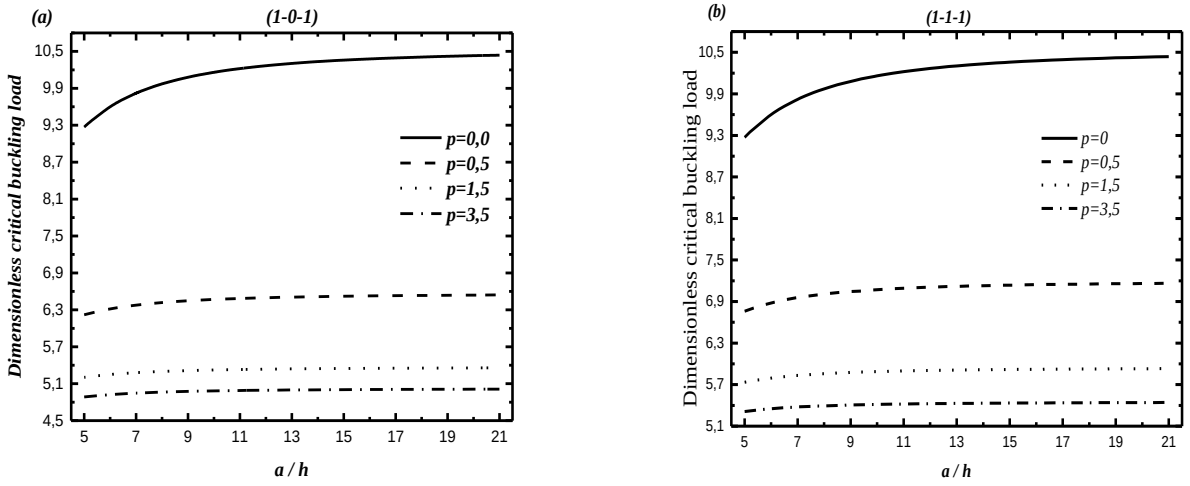

Fig. 4 Critical buckling versus the ratio a/h for various values of the inhomogeneity parameter p and various types of simply-supported EGM sandwich square plates resting on elastic foundations(k_w=k_s=10, χ=1)

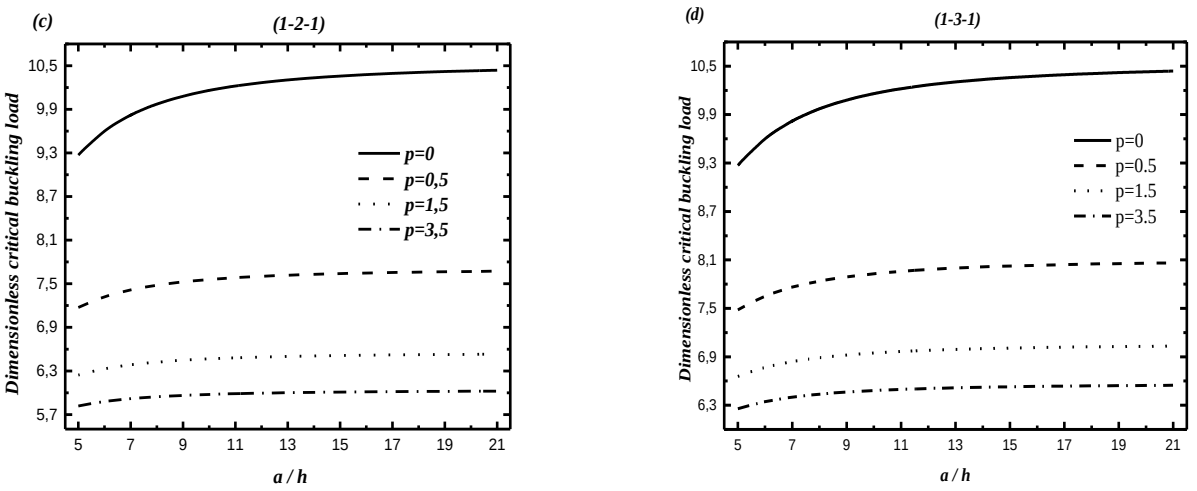

Fig. 4 Continued

Table 6 Effects of inhomogeneity parameter p and side-to-thickness ratio a/h on the critical buckling $\overline{N}_{cr}$ of (1-1-1) EGM sandwich plate (b/a=2, k_w=k_s=10)

B.C	Theory	p=0			p=0.5			p=3.5		
		a/h=5	10	20	a/h=5	10	20	a/h=5	10	20
FFCC	FPT[a]	15.2693	204469	22.5889	10.5119	12.7398	13.5537	7.5375	8.449	8.7524
	TPT[a]	15.3100	20.4524	22.5893	10.7685	12.8483	13.5856	7.5375	8.5326	8.7755
	SPT[a]	15.3262	20.4573	22.5906	10.7791	12.8519	13.5866	7.7767	8.5375	8.7769
	EPT[a]	15.3581	20.4701	22.5943	10.7947	12.8576	13.5882	7.7922	8.5427	8.7783
	HPT[a]	16.4396	21.0333	22.7718	10.9820	12.9404	13.6126	7.7130	8.5156	8.7709
	Present	15.2450	20.3388	22.5465	10.7129	12.8071	13.5722	7.7507	8.5248	8.7731
CCCC	FPT[a]	12.9480	15.8035	16.8213	8.9602	10.1273	10.5061	6.5737	7.0322	7.1710
	TPT[a]	12.9640	15.8053	16.8214	9.1032	10.1789	10.5205	6.6922	7.0708	7.1813
	SPT[a]	12.9719	15.8075	16.8220	9.1086	10.1806	10.5209	6.6994	7.0730	7.1819
	EPT[a]	12.9892	15.8136	16.8237	9.1167	10.1833	10.5216	6.7073	7.0754	7.1826
	HPT[a]	13.6482	16.0906	16.9044	9.2238	10.2228	10.5326	6.6669	7.0629	7.1792
	Present	12.7312	15.6712	16.7793	8.9957	10.1326	10.5071	6.6584	7.0585	7.1780
CSCS	FPT[a]	10.8802	12.4597	12.9692	7.6668	8.2896	8.4768	5.8071	6.0450	6.1130
	TPT[a]	10.8866	12.4603	12.9692	7.7464	8.3154	8.4837	5.8704	6.0641	6.1180
	SPT[a]	10.8906	12.4613	12.9695	7.7493	8.3163	8.4840	5.8742	6.0652	6.1183
	EPT[a]	10.9001	12.4644	12.9703	7.7536	8.3176	8.4843	5.8783	6.0663	6.1186
	HPT[a]	11.2895	12.6060	13.0096	7.8139	8.3374	8.4896	5.8572	6.0602	6.1170
	Present	10.8985	12.4516	12.9659	7.7465	8.3127	8.4829	5.8740	6.0646	6.1181
CCSS	FPT[a]	12.7243	15.4988	16.4857	8.8365	9.9698	10.3370	6.5105	6.9555	7.0900
	TPT[a]	12.7293	15.5004	16.4858	8.9755	10.0199	10.3509	6.6256	6.9929	7.1000
	SPT[a]	12.7474	15.5026	16.4864	8.9808	10.0215	10.3514	6.6326	6.9950	7.1006
	EPT[a]	12.7642	15.5085	16.4880	8.9886	10.0241	10.3521	6.6402	6.9974	7.1012
	HPT[a]	13.4052	15.7773	16.5662	9.0927	10.0624	10.3627	6.6010	6.9853	7.0980
	Present	12.6595	15.4643	16.4752	8.9458	10.0089	10.3479	6.6239	6.9923	7.0999
CSSS	FPT[a]	10.6131	12.0668	12.5311	7.5143	8.0853	8.2557	5.7275	5.9451	6.0069
	TPT[a]	10.6189	12.0673	12.5311	7.5876	8.1089	8.2620	5.7856	5.9624	6.0114
	SPT[a]	10.6225	12.0683	12.5314	7.5902	8.1096	8.2622	5.7891	5.9634	6.0117
	EPT[a]	10.6312	12.0711	12.5321	7.5942	8.1108	8.2625	5.7928	5.9645	6.0120

Table 6 Continued

B.C	Theory	p=0			p=0.5			p=3.5		
		a/h=5	10	20	a/h=5	10	20	a/h=5	10	20
CSSS	HPT[a]	10.9920	12.2004	12.5678	7.6497	8.1289	8.2674	5.7735	5.9589	6.0105
	Present	10.6225	12.0631	12.5296	7.5883	8.1080	8.2617	5.7899	5.9635	6.0117
SSSS	FPT[a]	7.5245	7.9088	8.0175	5.7741	5.9182	5.9575	4.8112	4.8643	4.8784
	TPT[a]	7.5252	7.9089	8.0175	5.7935	5.9237	5.9590	4.8259	4.8683	4.8795
	SPT[a]	7.5261	7.9091	8.0175	5.7942	5.9239	5.9590	4.8267	4.8685	4.8795
	EPT[a]	7.5284	7.9097	8.0177	5.7952	5.9242	5.9591	4.8277	4.8688	4.8796
	HPT[a]	7.6317	7.9407	8.0258	5.8101	5.9284	5.9602	4.8229	4.8675	4.8792
	Present	7.5281	7.9097	8.0177	5.7951	5.9242	5.9591	4.8276	4.8688	4.8796

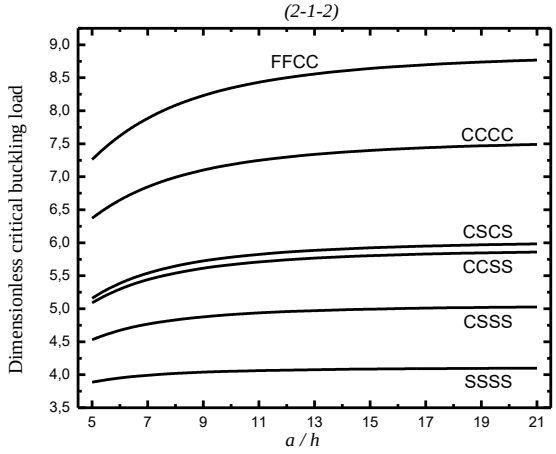

Fig. 5 Critical buckling $\overline{N}_{cr}$ versus the side-to-thickness ratio a/h of the (2-1-2) EGM sandwich square plate resting on Winkler's elastic foundation with various boundary conditions (k_w=100, p=1, χ=1)

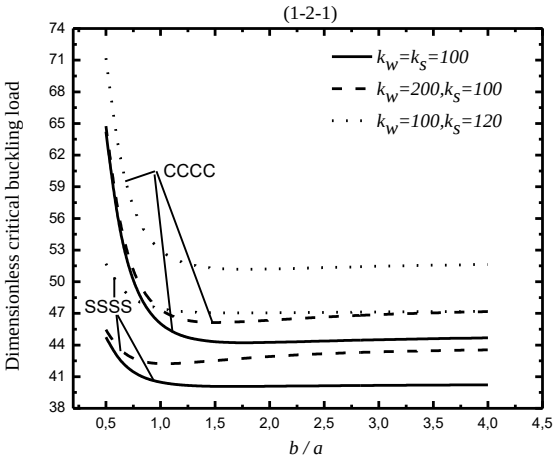

Fig. 6 Critical buckling versus the aspect ratio b/a of simply-supported and clamped sandwich plate for different values of foundation stiffnesses k_w and k_s (a/h=10, p=0.5, χ=1)

Table 5 give the effects of elastic foundation stiffnesses k_w and k_s and side-to-thickness ratio a/h on the critical buckling $\overline{N}_{cr}$ of various types of simply supported sandwich square plates (p = 0.5). The results are compared with those obtained using various shear deformation plate theories (Sobhi 2013) such as the FPT, the third-order shear deformation plate theory, the sinusoidal shear deformation plate theory, the exponential shear deformation plate theory, and the hyperbolic shear deformation plate theory. Good agreement is achieved between the present solutions using a new four-unknown refined plate theory and the published ones. It can be observed from Table 5 that the increase of the core thickness of the EGM sandwich plates leads to the increase of the buckling load, except for the case of the plates resting on Pasternak's foundations where the variation of them is reversed. In addition, the buckling load is increasing with the existence of the elastic foundations.

The inclusion of the Pasternak's foundation parameters gives results more than those with the inclusion of Winkler's foundation parameter.

Table 6 contains critical buckling load of the (1–1–1) EGM sandwich plate resting on two-parameter elastic foundations under various boundary conditions. The obtained results are compared with those reported by Sobhy (2013) for different values of the side-to-thickness ratio a/h and inhomogeneity parameter p. It can be seen that the results obtained in this study using a new four-unknown refined plate theory is in good agreement with the solutions given by Sobhy (2013). A decrement for the critical buckling load can be clearly observed with the increase of the parameter p. The results are maximum for the free-clamped plates and minimum for the simply supported plates.

The inclusion of the Pasternak's foundation parameters gives results more than those with the inclusion of Winkler's foundation parameter.

Table 6 contains critical buckling load of the (1–1–1) EGM sandwich plate resting on two-parameter elastic foundations under various boundary conditions. The obtained results are compared with those reported by Sobhy (2013) for different values of the side-to-thickness ratio a/h and inhomogeneity parameter p. It can be seen that the results obtained in this study using a new four-unknown refined plate theory is in good agreement with the solutions given by Sobhy (2013). A decrement for the critical buckling load can be clearly observed with the increase of the parameter p. The results are maximum for the free-clamped plates and minimum for the simply supported plates.

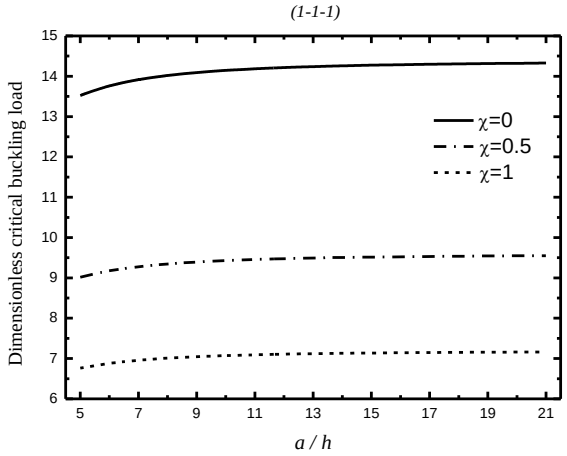

Fig. 7 Critical buckling versus the side-to-thickness ratio a/h of simply-supported sandwich square plate for different values of χ (k_w=k_s=10, p=0.5)

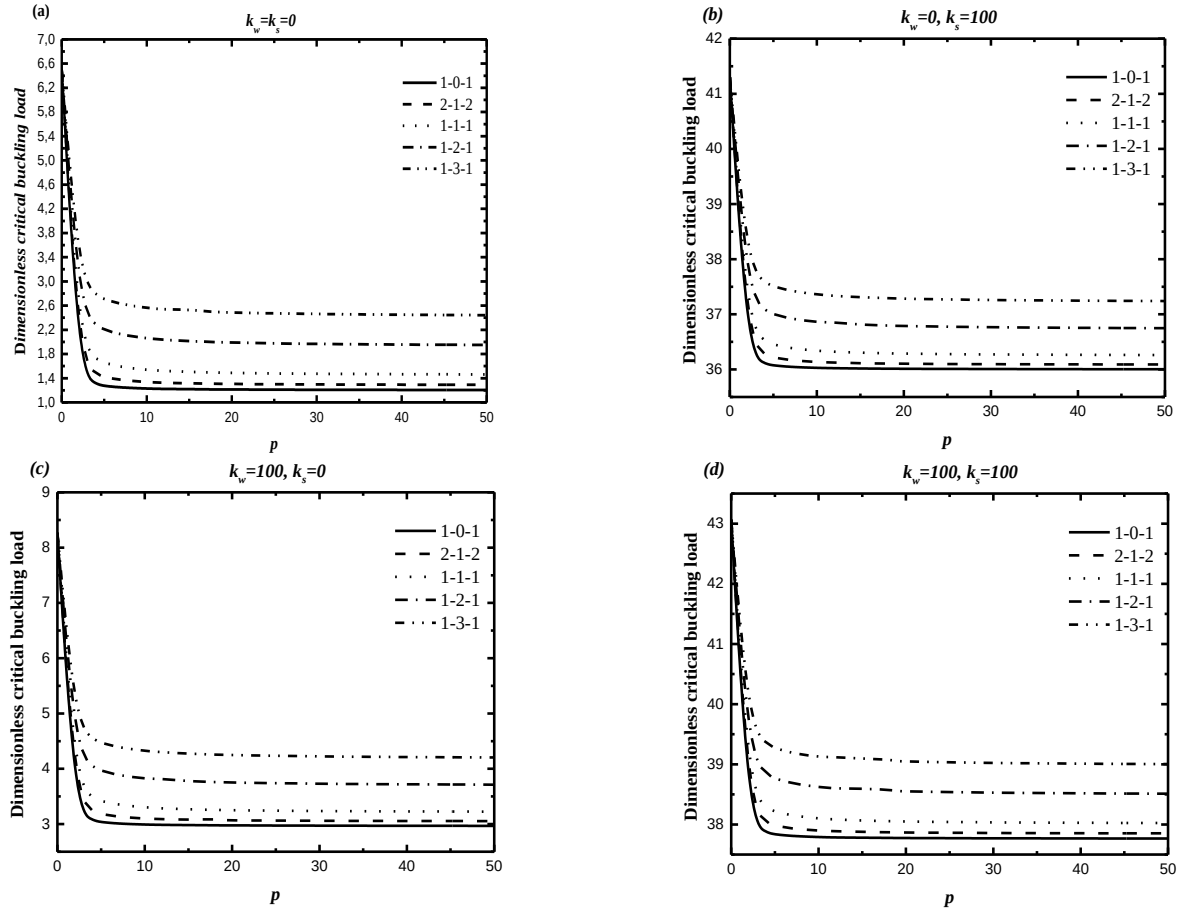

Fig. 8 Effect of power law index p on dimensionless critical buckling load of simply-supported sandwich square plates under biaxial compression for different values of foundation stiffnesses k_w and k_s (χ=1, a = 10 h)

Fig. 4 displays the variations of the critical buckling loads $\overline{N}_{cr}$ versus the side-to-thickness ratio a/h for different values of the inhomogeneity parameter p. It can be seen that the buckling loads increase monotonically as p decreases. It is observed that the differences between curves are reduced as the core thickness increases. It is also shown that the critical buckling load decreases as the volume fraction index p increase.

Fig. 5 present the critical buckling loads $\overline{N}_{cr}$ of (2–1–2) EGM sandwich square plate resting on Winkler's elastic foundation with various boundary conditions. It is noted that $\overline{N}_{cr}$ increase gradually as the side-to-thickness ratio a/h increases. The results of the simply supported sandwich plate are less than that of the clamped-clamped and free-clamped sandwich plate.

For the EGM sandwich plate with intermediate

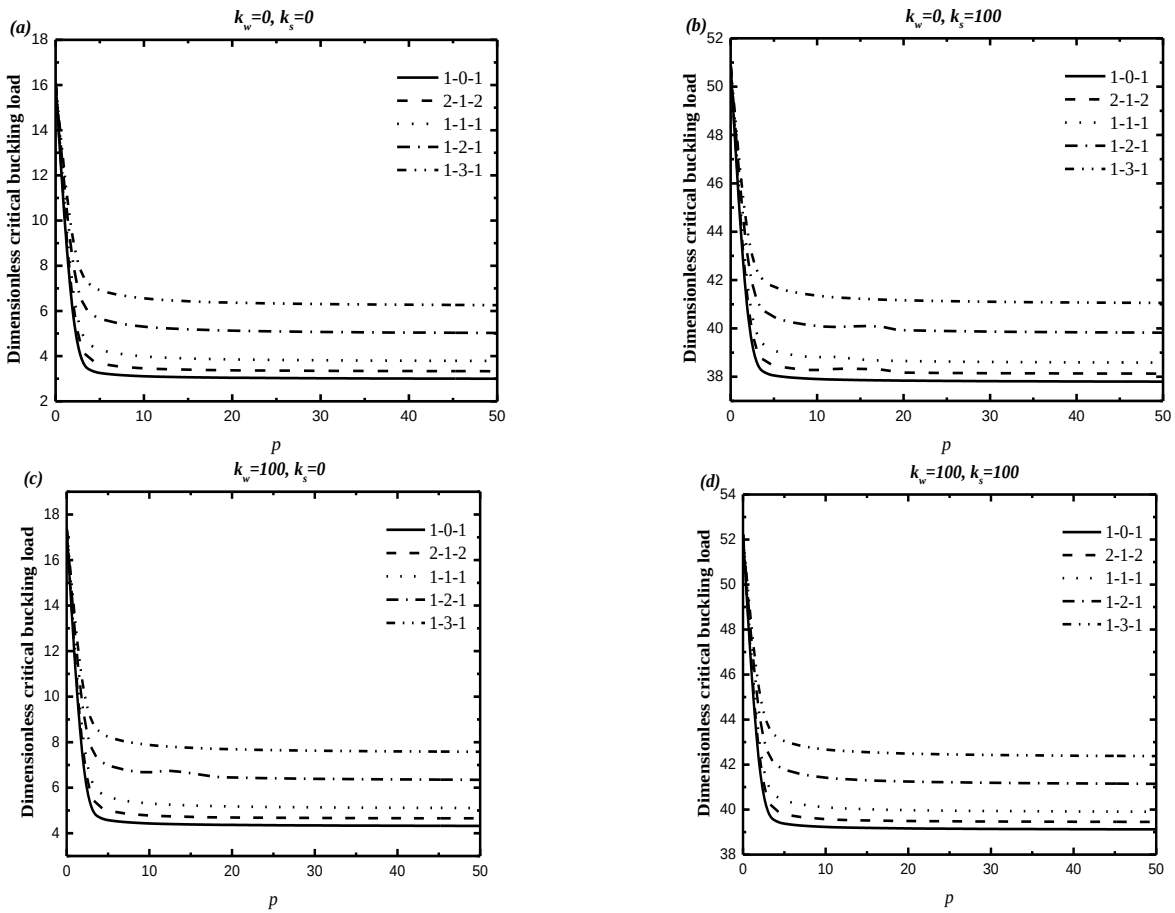

Fig. 9 Effect of power law index p on dimensionless critical buckling load of clamped sandwich square plates under biaxial compression for different values of foundation stiffnesses k_w and k_s (k_w, a = 10h)

boundary conditions, the results take the corresponding intermediate values.

Fig. 6 illustrates the variations of the buckling loads as functions of the aspect ratio b/a of the SSSS and CCCC plate for various values of the elastic foundation parameters. As it is well known, the clamped boundary condition always overpredicts the buckling loads magnitude. It can be noticed that the effect of the ratio b/a on the frequencies and the buckling loads is not the same. The buckling loads decrease rabidly and then increase very slowly as b/a increases. Obviously, the buckling loads are increasing with the increasing of the foundation stiffnesses.

Finally, the influence of the parameter χ on the critical buckling loads $\overline{N}_{cr}$ is demonstrated in Fig. 7. As expected, the uniaxial buckling load ($\chi = 0$) is greater than the biaxial one ($\chi > 0$) and that decreases as the parameter χ increases.

The effects of the power law index p on critical buckling load of SSSS and CCCC FG sandwich square plates under biaxial compression for different values of foundation stiffnesses k_w and k_s are illustrated in Figs. 8 and 9, respectively. The thickness ratio of the plate is taken equal to 10.It can be seen that increasing the power law index p results in an increase a reduction of buckling load. This is due to the fact that higher power law index p corresponds to lower volume fraction of the ceramic phase. In other word, increasing the power law index will reduce the stiffness of the plate due to high portion of metal in comparison with the ceramic part, and consequently, leads to a reduction of buckling load. Obviously, both the buckling loads are increasing with the increasing of the foundation stiffnesses.

5. Conclusions

A new shear deformation theory for buckling response of various types of EGM sandwich plates with different cases of boundary conditions is proposed in this paper. It contains only four unknowns, accounts for a hyperbolic distribution of transverse shear stress and satisfies the traction free boundary conditions. The sandwiches plates are assumed to be leaned on two-parameter elastic foundations. The governing equations are obtained through the principle of virtual work. To solve the buckling problem for different boundary conditions, Galerkin's approach is utilized for symmetric EGM sandwich plates with six different boundary conditions. Obtained results were presented in figures and tables and compared with references and these demonstrate the accuracy of present approach. Based on the results obtained, the following conclusions can be drawn from the present analysis:

1. The present results are very agreement with those being in literature.

2. The critical buckling loads increases as the side-to-thickness ratio a/h increases.

3. The critical buckling load of EGM sandwich plate

increases as the plate aspect ratio a/b decreases.

4. The foundation stiffness has a significant effect on the buckling load of sandwich plates. The effect of the k_s on the critical buckling loads is more pronounced than k_s.

5. In Fig. 4 it is shown that the critical buckling load decreases as the volume fraction index p increases.

6. The buckling loads for EGM sandwich plates are generally lower than the corresponding values for homogeneous ceramic plates.

7. The buckling loads for simply-supported EGM sandwich plates are lower than those for free and clamped EGM sandwich plates.

8. The critical buckling load for the plate under uniaxial compression is greater than the plate under biaxial compression.

Finally, an improvement of the present formulation will be considered in the future work to consider other type of structures and materials (Sedighi *et al.* 2012, 2013 and 2015, Arani and Kolahchi 2016, Bilouei *et al.* 2016, Kolahchi *et al.* 2016a, b, c and 2017b, Akbas 2017a, Motezaker and Kolahchi 2017a, b, Zarei *et al.* 2017, Zamanian *et al.* 2017, Amnieh *et al.* 2018, Behera and Kumari 2018, Panjehpour *et al.* 2018, Abdou *et al.* 2019, Hieu and Hai 2019, Malikan 2019, Selmi 2019, Othman *et al.* 2019, Jamali *et al.* 2019, Ayat *et al.* 2018, Eltaher and Wagih 2020, Amir Arbabi *et al.* 2020, Kolahchi *et al.* 2020a, b, Motezaker and Eyvazian 2020a, b, Timesli 2020, Motezaker *et al.* 2020).

References

Abdelmalek, A., Bouazza, M., Zidour, M. and Benseddiq, N. (2019), "Hygrothermal effects on the free vibration behavior of composite plate using nth-order shear deformation theory: A Micromechanical approach", *Iran. J. Sci. Technol. Trans. Mech. Eng.*, **43**, 61-73. https://doi.org/10.1007/s40997-017-0140-y.

Abdou, M.A., Othman, M.I.A., Tantawi, R.S. and Mansour, N.T. (2019), "Exact solutions of generalized thermoelastic medium with double porosity under L–S theory", *Indian J. Phys.*, 1-12. https://doi.org/10.1007/s12648-019-01505-8.

Ahmed, R.A., Fenjan, R.M. and Faleh, N.M. (2019), "Analyzing post-buckling behavior of continuously graded FG nanobeams with geometrical imperfections", *Geomech. Eng.*, **17**(2), 175-180. https://doi.org/10.12989/gae.2019.17.2.175.

Akbaş, S.D (2017a), "Nonlinear static analysis of functionally graded porous beams under thermal effect", *Coupled Syst. Mech.*, **6**(4), 399-415. https://doi.org/10.12989/csm.2017.6.4.399.

Akbas, S.D. (2019a), "Hygro-thermal post-buckling analysis of a functionally graded beam", *Coupled Syst. Mech.*, **8**(5), 459-471. https://doi.org/10.12989/csm.2019.8.5.459.

Akbas, S.D. (2019b), "Forced vibration analysis of functionally graded sandwich deep beams", *Coupled Syst. Mech.*, **8**(3), 259-271. https://doi.org/10.12989/csm.2019.8.3.259.

Al-Maliki, A.F.H., Faleh, N.M., Abbas, A. and Alasadi, A.A. (2019), "Finite element formulation and vibration of nonlocal refined metal foam beams with symmetric and non-symmetric porosities", *Struct. Monit. Maint.*, **6**(2), 147-159. https://doi.org/10.12989/smm.2019.6.2.147.

Alasadi, A.A., Ahmed, R.A. and Faleh, N.M. (2019), "Analyzing nonlinear vibrations of metal foam nanobeams with symmetric and non-symmetric porosities", *Adv. Aircraft Spacecraft Sci.*, **6**(4), 273-282. https://doi.org/10.12989/aas.2019.6.4.273.

Amnieh, H.B., Zamzam, M.S. and Kolahchi, R. (2018), "Dynamic analysis of non-homogeneous concrete blocks mixed by SiO2 nanoparticles subjected to blast load experimentally and theoretically", *Construct. Build. Mater.*, **174**, 633-644. https://doi.org/10.1016/j.conbuildmat.2018.04.140.

Anderson, T.A. (2003), "A 3-D elasticity solution for a sandwich composite with functionally graded core subjected to transverse loading by a rigid sphere", *Compos. Struct.*, **60**(3), 265-274. https://doi.org/10.1016/s0263-8223(03)00013-8.

Arani, A.J. and Kolahchi, R. (2016), "Buckling analysis of embedded concrete columns armed with carbon nanotubes", *Comput. Concrete*, **17**(5), 567-578. https://doi.org/10.12989/cac.2016.17.5.567.

Arbabi, A., Kolahchi, R. and Bidgoli, M.R, (2020), "Experimental study for ZnO nanofibers effect on the smart and mechanical properties of concrete", *Smart Struct. Syst.*, **25**(1), 97-104. https://doi.org/10.12989/sss.2020.25.1.097.

Avcar, M. (2019), "Free vibration of imperfect sigmoid and power law functionally graded beams", *Steel Compos. Struct.*, **30**(6), 603-615. https://doi.org/10.12989/scs.2019.30.6.603.

Ayat, H., Kellouche, Y., Ghrici, M. and Boukhatem, B. (2018), "Compressive strength prediction of limestone filler concrete using artificial neural networks", *Adv. Comput. Des.*, **3**(3), 289-302. https://doi.org/10.12989/acd.2018.3.3.289.

Azmi, M., Kolahchi, R. and Bidgoli, M.R. (2019), "Dynamic analysis of concrete column reinforced with Sio2 nanoparticles subjected to blast load", *Adv. Concrete Construct.*, **7**(1), 51-63. https://doi.org/10.12989/acc.2019.7.1.051.

Barati, M.R. and Shahverdi, H. (2020), "Finite element forced vibration analysis of refined shear deformable nanocomposite graphene platelet-reinforced beams", *J. Braz. Soc. Mech. Sci. Eng.*, **42**(1), 33. https://doi.org/10.1007/s40430-019-2118-8.

Behera, S. and Kumari, P. (2018), "Free vibration of Levy-type rectangular laminated plates using efficient zig-zag theory", *Adv. Comput. Des.*, **3**(3), 213-232. https://doi.org/10.12989/acd.2017.2.3.165.

Behravan Rad, A. (2012), "Static response of 2-D functionally graded circular plate with gradient thickness and elastic foundations to compound loads", *Struct. Eng. Mech.*, **44**(2), 139-161. https://doi.org/10.12989/sem.2012.44.2.139.

Belkacem, A., Tahar, H. D., Abderrezak, R., Amine, B.M., Mohamed, Z. and Boussad, A. (2018), "Mechanical buckling analysis of hybrid laminated composite plates under different boundary conditions", *Struct. Eng. Mech.*, **66**(6), 761-769. https://doi.org/10.12989/sem.2018.66.6.761.

Bilouei, B.S., Kolahchi, R. and Bidgoli, M.R. (2016), "Buckling of concrete columns retrofitted with nano-fiber reinforced Polymer (NFRP)", *Comput. Concrete*, **18**(5), 1053-1063. https://doi.org/10.12989/cac.2016.18.6.1053.

Das, M., Barut, A., Madenci, E. and Ambur, D.R. (2006), "A triangular plate element for thermo-elastic analysis of sandwich panels with a functionally graded core", *Int. J. Numer. Meth. Eng.*, **68**(9), 940-966. https://doi.org/10.1002/nme.1724.

Ebrahimi, F. and Barati, M.R. (2018), "Hygro-thermal vibration analysis of bilayer graphene sheet system via nonlocal strain gradient plate theory", *J. Braz. Soc. Mech. Sci. Eng.*, **40**(9), 428. https://doi.org/10.1007/s40430-018-1350-y.

Ebrahimi, F. and Barati, M.R. (2019), "A nonlocal strain gradient mass sensor based on vibrating hygro-thermally affected graphene nanosheets", *Iran. J. Sci. Technol. Trans. Mech. Eng.*, **43**, 205-220. https://doi.org/10.1007/s40997-017-0131-z.

Ebrahimi, F., Barati, M.R. and Civalek, Ö. (2019), "Application of Chebyshev–Ritz method for static stability and vibration analysis of nonlocal microstructure-dependent nanostructures", *Eng. Comput.*, 1-12. https://doi.org/10.1007/s00366-019-00742-z.

Eltaher, M.A. and Mohamed, S.A. (2020), "Buckling and stability analysis of sandwich beams subjected to varying axial loads",

Steel Compos. Struct., **34**(2), 241-260. https://doi.org/10.12989/scs.2020.34.2.241.

Eltaher, M.A. and Wagih, A. (2020), "Micromechanical modeling of damage in elasto-plastic nanocomposites using unit cell representative volume element and cohesive zone model", *Ceramics Int*. https://doi.org/10.1016/j.ceramint.2020.01.046.

Fakhar, A. and Kolahchi, R. (2018), "Dynamic buckling of magnetorheological fluid integrated by visco-piezo-GPL reinforced plates", *Int. J. Mech. Sci.*, **144**, 788-799. https://doi.org/10.1016/j.ijmecsci.2018.06.036.

Farrokhian, A. and Kolahchi, R. (2020), "Frequency and instability responses in nanocomposite plate assuming different distribution of CNTs", *Struct. Eng. Mech.*, **73**(5), 555-563. https://doi.org/10.12989/sem.2020.73.5.555.

Fenjan, R.M., Ahmed, R.A., Alasadi, A.A. and Faleh, N.M. (2019), "Nonlocal strain gradient thermal vibration analysis of double-coupled metal foam plate system with uniform and non-uniform porosities", *Coupled Syst. Mech.*, **8**(3), 247-257. https://doi.org/10.12989/csm.2019.8.3.247.

Filipich, C.P. and Rosales, M.B. (2002), "A further study about the behaviour of foundation piles and beams in a Winkler-Pasternak soil", *Int. J. Mech. Sci.*, **44**(1), 21-36. https://doi.org/10.1016/s0020-7403(01)00087-x.

Golabchi, H., Kolahchi, R. and Bidgoli, M.R. (2018), "Vibration and instability analysis of pipes reinforced by SiO2 nanoparticles considering agglomeration effects", *Comput. Concrete*, **21**(4), 431-440. https://doi.org/10.12989/cac.2018.21.4.431.

Hadji, L., Zouatnia, N. and Bernard, F. (2019), "An analytical solution for bending and free vibration responses of functionally graded beams with porosities: Effect of the micromechanical models", *Struct. Eng. Mech.*, **69**(2), 231-241. https://doi.org/10.12989/sem.2019.69.2.231.

Hajmohammad, M.H., Farrokhian, A. and Kolahchi, R. (2018a), "Smart control and vibration of viscoelastic actuator-multiphase nanocomposite conical shells-sensor considering hygrothermal load based on layerwise theory", *Aerosp. Sci. Technol.*, **78**, 260-270. https://doi.org/10.1016/j.ast.2018.04.030.

Hajmohammad, M.H., Kolahchi, R., Zarei, M.S. and Maleki, M. (2018c), "Earthquake induced dynamic deflection of submerged viscoelastic cylindrical shell reinforced by agglomerated CNTs considering thermal and moisture effects", *Compos. Struct.*, **187**, 498-508. https://doi.org/10.1016/j.compstruct.2017.12.004.

Hajmohammad, M.H., Kolahchi, R., Zarei, M.S. and Nouri, A.H. (2019), "Dynamic response of auxetic honeycomb plates integrated with agglomerated CNT-reinforced face sheets subjected to blast load based on visco-sinusoidal theory", *Int. J. Mech. Sci.*, **153**, 391-401. https://doi.org/10.1016/j.ijmecsci.2019.02.008.

Hajmohammad, M.H., Maleki, M. and Kolahchi, R. (2018b), "Seismic response of underwater concrete pipes conveying fluid covered with nano-fiber reinforced polymer layer", *Soil Dyn. Earthq. Eng.*, **110**, 18-27. https://doi.org/10.1016/j.soildyn.2018.04.002.

Hajmohammad, M.H., Zarei, M.S., Nouri, A. and Kolahchi, R. (2017), "Dynamic buckling of sensor/functionally graded-carbon nanotube-reinforced laminated plates/actuator based on sinusoidal-visco-piezoelasticity theories", *J. Sandw. Struct. Mater.* https://doi.org/10.1177/1099636217720373.

Hamed, M.A., Mohamed, S.A. and Eltaher, M.A. (2020), "Buckling analysis of sandwich beam rested on elastic foundation and subjected to varying axial in-plane loads", *Steel Compos. Struct.*, **34**(1), 75-89. https://doi.org/10.12989/scs.2020.34.1.075.

Hamidi, A., Zidour, M., Bouakkaz, K. and Bensattalah, T. (2018), "Thermal and small-scale effects on vibration of embedded armchair single-walled carbon nanotubes", *J. Nano Res.*, **51**, 24-38. https://doi.org/10.4028/www.scientific.net/JNanoR.51.24.

Hieu, D. and Hai, N.Q. (2019), "Free vibration analysis of quintic nonlinear beams using equivalent linearization method with a weighted averaging", *J. Appl. Comput. Mech.*, **5**(1), 46-57. https://doi.org/10.22055/jacm.2018.24919.1217.

Hosseini, H. and Kolahchi, R. (2018), "Seismic response of functionally graded-carbon nanotubes-reinforced submerged viscoelastic cylindrical shell in hygrothermal environment", *Physica E Low-dimens. Syst. Nanostruct.*, **102**, 101-109. https://doi.org/10.1016/j.physe.2018.04.037.

Jamali, M., Shojaee, T., Mohammadi, B. and Kolahchi, R. (2019), "Cut out effect on nonlinear post-buckling behavior of FG-CNTRC micro plate subjected to magnetic field via FSDT", *Adv. Nano Res.*, **7**(6), 405-417. https://doi.org/10.12989/anr.2019.7.6.405.

Katariya, P.V., Panda, S.K. and Mahapatra, T.R. (2017), "Prediction of nonlinear eigen frequency of laminated curved sandwich structure using higher-order equivalent single-layer theory", *J. Sandw. Struct. Mater.*, 109963621772842. https://doi.org/10.1177/1099636217728420.

Keshtegar, B., Bagheri, M., Meng, D., Kolahchi, R. and Trung, N.T. (2020a), "Fuzzy reliability analysis of nanocomposite ZnO beams using hybrid analytical-intelligent method", *Eng. Comput.*, 1-16. https://doi.org/10.1007/s00366-020-00965-5.

Keshtegar, B., Tabatabaei, J., Kolahchi, R. and Trung, N.T. (2020b), "Dynamic stress response in the nanocomposite concrete pipes with internal fluid under the ground motion load", *Adv. Concrete Construct.*, **9**(3), 327-335. https://doi.org/10.12989/acc.2020.9.3.327.

Koizumi M. (1997), "FGM activities in Japan", *Compos. Part B Eng.*, **28**(1-2), 1-4. https://doi.org/10.1016/S1359-8368(96)00016-9.

Kolahchi, R. (2017), "A comparative study on the bending, vibration and buckling of viscoelastic sandwich nano-plates based on different nonlocal theories using DC, HDQ and DQ methods", *Aerosp. Sci. Technol.*, **66**, 235-248. https://doi.org/10.1016/j.ast.2017.03.016.

Kolahchi, R. and Cheraghbak, A. (2017), "Agglomeration effects on the dynamic buckling of viscoelastic microplates reinforced with SWCNTs using Bolotin method", *Nonlin. Dyn.*, **90**, 479-492. https://doi.org/10.1007/s11071-017-3676-x.

Kolahchi, R., Hosseini, H., Fakhar, M.H., Taherifar, R. and Mahmoudi, M. (2019), "A numerical method for magneto-hygro-thermal postbuckling analysis of defective quadrilateral graphene sheets using higher order nonlocal strain gradient theory with different movable boundary conditions", *Comput. Math. Appl.*, **78**(6), 2018-2034. https://doi.org/10.1016/j.camwa.2019.03.042.

Kolahchi, R., Keshtegar, B. and Fakhar, M.H. (2020a), "Optimization of dynamic buckling for sandwich nanocomposite plates with sensor and actuator layer based on sinusoidal-visco-piezoelasticity theories using Grey Wolf algorithm", *J. Sandw. Struct. Mater.*, **22**(1). https://doi.org/10.1177/1099636217731071.

Kolahchi, R. and Moniri Bidgoli, A.M. (2016), "Size-dependent sinusoidal beam model for dynamic instability of single-walled carbon nanotubes", *Appl. Math. Mech. Engl. Ed.*, **37**, 265-274. https://doi.org/10.1007/s10483-016-2030-8.

Kolahchi, R., Zarei, M.S., Hajmohammad, M.H. and Nouri, A. (2017b), "Wave propagation of embedded viscoelastic FG-CNT-reinforced sandwich plates integrated with sensor and actuator based on refined zigzag theory", *Int. J. Mech. Sci.*, **130**, 534-545. https://doi.org/10.1016/j.ijmecsci.2017.06.039.

Kolahchi, R., Zarei, M.S., Hajmohammad, M.H. and Oskouei, A.N. (2017a), "Visco-nonlocal-refined Zigzag theories for dynamic buckling of laminated nanoplates using differential

cubature-Bolotin methods", *Thin-Walled Struct*., **113**, 162-169. https://doi.org/10.1016/j.tws.2017.01.016.

Kolahchi, R., Zhu, S.P., Keshtegar, B. and Trung, N.T. (2020b), "Dynamic buckling optimization of laminated aircraft conical shells with hybrid nanocomposite martial", *Aerosp. Sci. Technol*., **98**, 105656. https://doi.org/10.1016/j.ast.2019.105656.

Kolahchi, R., Hosseini, H. and Esmailpour, M. (2016b), "Differential cubature and quadrature-Bolotin methods for dynamic stability of embedded piezoelectric nanoplates based on visco-nonlocal-piezoelasticity theories", *Compos. Struct*., **157**, 174-186. https://doi.org/10.1016/j.compstruct.2016.08.032.

Kolahchi, R., Safari, M. and Esmailpour, M. (2016c), "Dynamic stability analysis of temperature-dependent functionally graded CNT-reinforced visco-plates resting on orthotropic elastomeric medium", *Compos. Struct*., **150**, 255-265. https://doi.org/10.1016/j.compstruct.2016.05.023.

Kolahchi, R., Safari, M. and Esmailpour, M. (2016a), "Dynamic stability analysis of temperature-dependent functionally graded CNT-reinforced visco-plates resting on orthotropic elastomeric medium", *Compos. Struct*., **150**, 255-265. https://doi.org/10.1016/j.ijmecsci.2017.06.039.

Li, Z.M. and Yang, D.Q. (2016), "Thermal postbuckling analysis of anisotropic laminated beams with tubular cross-section based on higher-order theory", *Ocean Eng*., **115**, 93-106. https://doi.org/10.1016/j.oceaneng.2016.02.017.

Madani, H., Hosseini, H. and Shokravi, M. (2016), "Differential cubature method for vibration analysis of embedded FG-CNT-reinforced piezoelectric cylindrical shells subjected to uniform and non-uniform temperature distributions", *Steel Compos. Struct*., **22**(4), 889-913. https://doi.org/10.12989/scs.2016.22.4.889.

Malikan, M. (2019), "On the buckling response of axially pressurized nanotubes based on a novel nonlocal beam theory", *J. Appl. Comput. Mech*., **5**(1), 103-112. https://doi.org/10.22055/jacm.2018.25507.1274.

Matsunaga, H. (2000), "Vibration and stability of thick plates on elastic foundations", *J. Eng. Mech*., **126**(1), 27-34. https://doi.org/10.1061/(ASCE)0733-9399(2000)126:1(27).

Matsunaga, H. (2008), "Free vibration and stability of functionally graded plates according to a 2-D higher-order deformation theory", *Compos. Struct*., **82**(4), 499-512. https://doi.org/10.1016/j.compstruct.2007.01.030.

Motezaker, M. and Eyvazian, A. (2020a), "Post-buckling analysis of Mindlin cut out-plate reinforced by FG-CNTs", *Steel Compos. Struct*., **34**(2), 289-297. https://doi.org/10.12989/scs.2020.34.2.289.

Motezaker, M. and Eyvazian, A. (2020b), "Buckling load optimization of beam reinforced by nanoparticles", *Struct. Eng. Mech*., **73**(5), 481-486. https://doi.org/10.12989/sem.2020.73.5.481.

Motezaker, M. and Kolahchi, R. (2017a), "Seismic response of concrete columns with nanofiber reinforced polymer layer", *Comput. Concrete*, **20**(3), 361-368. https://doi.org/10.12989/cac.2017.20.3.361.

Motezaker, M. and Kolahchi, R. (2017b), "Seismic response of SiO2 nanoparticles-reinforced concrete pipes based on DQ and newmark methods", *Comput. Concrete*, **19**(6), 745-753. https://doi.org/10.12989/cac.2017.19.6.745.

Motezaker, M., Jamali, M. and Kolahchi, R. (2020), "Application of differential cubature method for nonlocal vibration, buckling and bending response of annular nanoplates integrated by piezoelectric layers based on surface-higher order nonlocal-piezoelasticity theory", *J. Comput. Appl. Math*., **369**, 112625. https://doi.org/10.1016/j.cam.2019.112625.

Neves, A.M.A., Ferreira, A.J.M., Carrera, E., Cinefra, M., Jorge, R.M.N. and Soares, C.M.M. (2012e), "Buckling analysis of sandwich plates with functionally graded skins using a new quasi-3D hyperbolic sine shear deformation theory and collocation with radial basis functions", *ZAMM J. Appl. Math. Mech*., **92**(9), 749-766. https://doi.org/10.1002/zamm.201100186.

Neves, A.M.A., Ferreira, A.J.M., Carrera, E., Cinefra, M., Jorge, R.M.N. and Soares, C.M.M. (2012c), "Static analysis of functionally graded sandwich plates according to a hyperbolic theory considering Zig-Zag and warping effects", *Adv. Eng. Softw*., **52**, 30-43. https://doi.org/10.1016/j.advengsoft.2012.05.005.

Neves, A.M.A., Ferreira, A.J.M., Carrera, E., Cinefra, M., Jorge, R.M.N. and Soares, C.M.M. (2012b), "Buckling analysis of sandwich plates with functionally graded skins using a new quasi-3D hyperbolic sine shear deformation theory and collocation with radial basis functions", *ZAMM J. Appl. Math. Mech*., **92**(9), 749-766. https://doi.org/10.1002/zamm.201100186.

Neves, A.M.A., Ferreira, A.J.M., Carrera, E., Cinefra, M., Roque, C.M.C., Jorge, R.M.N. and Soares, C.M.M. (2012d), "A quasi-3D hyperbolic shear deformation theory for the static and free vibration analysis of functionally graded plates", *Compos. Struct*., **94**(5), 1814-1825. https://doi.org/10.1016/j.compstruct.2011.12.005.

Neves, A.M.A., Ferreira, A.J.M., Carrera, E., Roque, C.M.C., Cinefra, M., Jorge, R.M.N. and Soares, C.M.M. (2012a), "A quasi-3D sinusoidal shear deformation theory for the static and free vibration analysis of functionally graded plates", *Compos. Part B Eng*., **43**(2), 711-725. https://doi.org/10.1016/j.compositesb.2011.08.009.

Omurtag, M.H., Özütok, A., Aköz, A.Y. and Özçelikörs, Y. (1997), "Free vibration analysis of kirchhoff plates resting on elastic foundation by mixed finite element formulation based on gâteaux differential", *Int. J. Numer. Meth. Eng*., **40**(2), 295-317. https://doi.org/10.1002/(sici)1097-0207(19970130)40:2<295::aid-nme66>3.0.co;2-2.

Othman, M.I.A., Abouelregal, A.E. and Said, S.M. (2019), "The effect of variable thermal conductivity on an infinite fiber-reinforced thick plate under initial stress", *J. Mech. Mater. Struct*., **14**(2), 277-293. https://doi.org/10.2140/jomms.2019.14.277.

Panjehpour, M., Loh, E.W.K. and Deepak, TJ. (2018), "Structural Insulated Panels: State-of-the-Art", *Trends Civ. Eng. Architect*., **3**(1) 336-340. https://doi.org/10.32474/TCEIA.2018.03.000151.

Safa, A., Hadji, L., Bourada, M. and Zouatnia, N. (2019), "Thermal vibration analysis of FGM beams using an efficient shear deformation beam theory", *Earthq. Struct*., **17**(3), 329-336. https://doi.org/10.12989/eas.2019.17.3.329.

Sahouane, A., Hadji, L. and Bourada, M. (2019), "Numerical analysis for free vibration of functionally graded beams using an original HSDBT", *Earthq. Struct*., **17**(1), 31-37. https://doi.org/10.12989/eas.2019.17.1.031.

Sedighi, H.M. and Shirazi, K.H. (2012), "A new approach to analytical solution of cantilever beam vibration with nonlinear boundary condition", *J. Comput. Nonlin. Dyn.*, **7**(3), 034502. https://doi.org/10.1115/1.4005924.

Sedighi, H.M., Keivani, M. and Abadyan, M. (2015), "Modified continuum model for stability analysis of asymmetric FGM double-sided NEMS: Corrections due to finite conductivity, surface energy and nonlocal effect", *Compos. Part B Eng*., **83**, 117-133. https://doi.org/10.1016/j.compositesb.2015.08.029.

Sedighi, H.M., Shirazi, K.H. and Attarzadeh, M.A. (2013), "A study on the quintic nonlinear beam vibrations using asymptotic approximate approaches", *Acta Astronautica*, **91**, 245-250. https://doi.org/10.1016/j.actaastro.2013.06.018.

Selmi, A. (2019), "Effectiveness of SWNT in reducing the crack effect on the dynamic behavior of aluminium alloy", *Adv. Nano*

Res., **7**(5), 365-377. https://doi.org/10.12989/anr.2019.7.5.365.
Shen, H.S. and Yang, D.Q. (2014), "Nonlinear vibration of anisotropic laminated cylindrical shells with piezoelectric fiber reinforced composite actuators", *Ocean Eng*., **80**, 36-49. https://doi.org/10.1016/j.oceaneng.2014.01.016.
Shodja, H., Haftbaradaran, H. and Asghari, M. (2007), "A thermoelasticity solution of sandwich structures with functionally graded coating", *Compos*. *Sci*. *Technol*., **67**(6), 1073-1080. https://doi.org/10.1016/j.compscitech.2006.06.001.
Sobhy, M. (2013), "Buckling and free vibration of exponentially graded sandwich plates resting on elastic foundations under various boundary conditions", *Compos*. *Struct*, **99**, 76-87. https://doi.org/10.1016/j.compstruct.2012.11.018.
Timesli, A. (2020), "An efficient approach for prediction of the nonlocal critical buckling load of double-walled carbon nanotubes using the nonlocal Donnell shell theory", *SN Appl. Sci.*, **2**, 407. https://doi.org/10.1007/s42452-020-2182-9.
Wang, Z.X. and Shen, H.S. (2013), "Nonlinear dynamic response of sandwich plates with FGM face sheets resting on elastic foundations in thermal environments", *Ocean Eng*., **57**, 99-110. https://doi.org/10.1016/j.oceaneng.2012.09.004.
Xiang, S., Jin, Y., Bi, Z., Jiang, S. and Yang, M. (2011). "A n-order shear deformation theory for free vibration of functionally graded and composite sandwich plates", *Compos*. *Struct*., **93**(11), 2826-2832. https://doi.org/10.1016/j.compstruct.2011.05.022.
Yaghoobi, H. and Yaghoobi, P. (2013), "Buckling analysis of sandwich plates with FGM face sheets resting on elastic foundation with various boundary conditions: an analytical approach", *Meccanica*, **48**(8), 2019-2035. https://doi.org/10.1007/s11012-013-9720-0.
Zamanian, M., Kolahchi, R. and Bidgoli, M.R. (2017), "Agglomeration effects on the buckling behaviour of embedded concrete columns reinforced with SiO2 nano-particles", *Wind Struct*., **24**(1), 43-57. https://doi.org/10.12989/was.2017.24.1.043.
Zarei, M.S., Kolahchi, R., Hajmohammad, M.H. and Maleki, M. (2017), "Seismic response of underwater fluid-conveying concrete pipes reinforced with SiO2 nanoparticles and fiber reinforced polymer (FRP) layer", *Soil Dyn*. *Earthq*. *Eng*., **103**, 76-85. https://doi.org/10.1016/j.soildyn.2017.09.009.
Zenkour, A.M. (2005), "A comprehensive analysis of functionally graded sandwich plates: Part 2—Buckling and free vibration", *Int*. *J*. *Solids Struct*., **42**(18-19), 5243-5258. https://doi.org/10.1016/j.ijsolstr.2005.02.016.
Zenkour, A.M. and Alghamdi, N.A. (2008), "Thermoelastic bending analysis of functionally graded sandwich plates", *J*. *Mater*. *Sci*., **43**(8), 2574-2589. https://doi.org/10.1007/s10853-008-2476-6.
Zenkour, A.M. and Sobhy, M. (2010), "Thermal buckling of various types of FGM sandwich plates", *Compos*. *Struct*., **93**(1), 93-102. https://doi.org/10.1016/j.compstruct.2010.06.012.
Zhao, X., Lee, Y.Y. and Liew, K.M. (2009), "Mechanical and thermal buckling analysis of functionally graded plates", *Compos*. *Struct*., **90**(2), 161-171. https://doi.org/10.1016/j.compstruct.2009.03.005.
Zhou, D., Cheung, Y.K., Lo, S.H. and Au, F.T.K. (2004), "Three-dimensional vibration analysis of rectangular thick plates on Pasternak foundation", *Int*. *J*. *Numer*. *Meth*. *Eng.*, **59**(10), 1313–-334. https://doi.org/10.1002/nme.915.
Zouatnia, N. and Hadji, L. (2019), "Effect of the micromechanical models on the bending of FGM beam using a new hyperbolic shear deformation theory", *Earthq*. *Struct*., **16**(2), 177-183. https://doi.org/10.12989/eas.2019.16.2.177.